The phytoalexin, resveratrol ameliorates Ochratoxin A genotoxicity in Human Embryonic Kidney (HEK293)cells.

By

Shanel Raghubeer

B.Sc., B.Med.Sc. (Hons), (UKZN)

Submitted in fulfilment of the requirements for the degree M.Med.Sci in the discipline of Medical Biochemistry and Chemical Pathology

School of Laboratory Medicine and Medical Sciences

College of Health Sciences

University of Kwa-Zulu Natal

Durban

2014

Abstract

Background: Ochratoxin A (OTA) is a mycotoxin produced by fungal species of *Aspergillus* and *Penicillium.* OTA is nephrotoxic and carcinogenic in several animal models; it frequently contaminates human and animal food products. Chronic exposure is associated with progressive renal fibrosis in humans (Balkan endemic nephropathy). Resveratrol is a phytoalexin that possesses both anti-cancer and antioxidant properties. We investigated the mechanism of cellular oxidative stress induced by OTA in the human embryonic kidney (HEK293) cell line.

Methods: An IC_{50} value of 1.5µM was determined from a dose-dependent cell viability curve using the methylthiazol tetrazolium (MTT) assay on HEK293 cells treated with a range of OTA concentrations (0.25µM–50µM) for 24hrs. Glutathione levels were quantified by luminometry and gene expression of Nrf2, OGG1, CAT, SOD and GPx was determined by qPCR. Protein expression of Nrf2 and phosphorylated SIRT1 (pSIRT1) was assessed by western blot, DNA damage was determined using the comet assay, and flow cytometry was employed for intracellular ROS detection.

Results: Resveratrol decreased mRNA expression of OGG1 ($p<0.05$) and OTA significantly increased OGG1 expression ($p<0.05$). The comet assay proved that while OTA induced DNA damage, resveratrol protected the DNA against strand breaks. Both resveratrol and OTA significantly increased antioxidant defence gene expression (Nrf2, CAT, GPx and SOD) ($p<0.05$). OTA decreased intracellular ROS, while resveratrol-treated cells exhibited the lowest percentage of intracellular ROS. Luminometry analysis showed the OTA+Resveratrol co-treatment to have a synergistic effect on the concentration of GSH and GSSG. Western blot analysis of protein showed that resveratrol significantly increased the levels of pSIRT1 while

concomitantly decreasing the protein levels of Nrf2 (p<0.05) and OTA significantly decreased pSIRT1 protein levels.

Declaration

This dissertation contains the original work by the author and has not been submitted in any form to another university. The use of work by others has been duly acknowledged in the text.

The research described in this study was carried out in the division of Medical Biochemistry and Chemical Pathology, School of Laboratory Medicine and Medical Science, Faculty of Health Sciences, University of Kwa-Zulu Natal, Durban, under the supervision of Prof. A. A. Chuturgoon and Dr A. Phulukdaree.

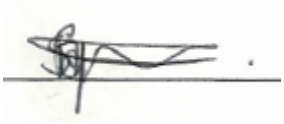

Miss S. Raghubeer

Acknowledgements

I would like to thank:

My Family

To my parents, thank you for affording me opportunities that you never had, for always supporting and encouraging me, and for providing guidance while allowing me to grow at my own pace. I am eternally grateful for all that you do for me. Thank you to my brother for encouraging me and keeping me grounded.

Friends and Loved ones

Thank you for your support and understanding, for being there for me when I needed a shoulder to cry on and for your ceaseless faith in me and my abilities. I treasure all of you.

Prof. A. A. Chuturgoon

Thank you for your guidance, your passion for science and for believing in me when I didn't believe in myself. You have inspired and motivated me more than anyone in my academic career and I appreciate you for that.

Dr A. Phulukdaree

For your tireless help and advice, I thank you. I would be lost without your supervision and guidance, your knowledge knows no bounds and I am very fortunate to have learned all that I have from you. You are an amazing teacher and mentor. Thank you.

The Medical Biochemistry Masters class of 2014

To the phenomenal women that I was lucky to spend this year with. Thank you for your friendship, your help in and out of the laboratory and your unwavering encouragement.

The PhD students and Staff of the Medical Biochemistry Department 2014

Thank you for all the assistance, guidance and patience I received. You have gone above and beyond your duties to help me and mould me into the scientist I am. Thank you for imparting your knowledge on me and teaching me something new every day.

NRF-DAAD

I would like to thank the NRF-DAAD for their financial support.

University of Kwa-Zulu Natal

I would like to thank UKZN for the financial support I received as a postgraduate student.

Publications

The following manuscript has been accepted for publication by the Journal of Cellular Biochemistry.

Manuscript number: JCB-14-0585

S. Raghubeer, S. Nagiah, A. Phulukdaree and A.A Chuturgoon. The phytoalexin, Resveratrol ameliorates Ochratoxin A toxicity in Human Embryonic Kidney (HEK293) cells.

Presentations

1) The effects of Oxidative Stress induction by Ochratoxin A on Human Embryonic Kidney (HEK293) cells.

Raghubeer S., Phulukdaree A., Chuturgoon A.A.

UKZN School of Laboratory Medicine and Medical Science Research Symposium (May, 2014), Durban, South Africa

2) The effects of Oxidative Stress induction by Ochratoxin A on Human Embryonic Kidney (HEK293) cells.

Raghubeer S., Phulukdaree A., Chuturgoon A.A.

UKZN College of Health Science Research Symposium (September, 2014), Durban, South Africa

List of Abbreviations

˚C	Degrees Celsius
ANOVA	Analysis of variance
ARE	Antioxidant response element
BCA	Bicinchoninic acid
BEN	Balkan Endemic Nephropathy
BER	Base excision repair
BSA	Bovine serum albumin
Ca^{2+}	Calcium
CAT	Catalase
CCM	Complete culture medium
cDNA	Complementary DNA
CHD	Coronary heart disease
CO_2	Carbon dioxide
COX	Cyclooxygenase
CR	Calorie restriction
Cu^{1+}	Cuprous ions
Cu^{2+}	Copper
$CuSO_4$	Copper sulphate
CYP_{450}	Cytochrome P_{450}
DCF	2', 7'-dichlorofluorescein
DCFDA	Dichlorohydrofluorescein diacetate
DMEM	Dulbecco's minimum essential media
DMSO	Dimethyl sulphoxide

DNA	Deoxyribonucleic acid
dNTP	Deoxynucleoside triphosphate
dsDNA	Double stranded DNA
EDTA	Ethylenediaminetetraacetic acid
ER	Endoplasmic reticulum
ETC	Electron transport chain
FACS	Fluorescence activated cell sorting
FCS	Foetal calf serum
Fe^{2+}	Iron
g	Gravitational force
G6PD	Glucose-6-phosphate dehydrogenase
GIT	Gastrointestinal tract
GPx	Glutathione peroxidase
GR	Glutathione reductase
GSH	Glutathione
GSSG	Glutathione disulfide
GST	Glutathione S-transferase
H^+	Hydrogen
H_2O_2	Hydrogen peroxide
HEK293	Human embryonic kidney
HRP	Horseradish peroxidase
Hrs	Hours
IC_{50}	Half maximal inhibitory concentration
Keap1	Kelch-like ECH-associated protein1
LDL	Low density lipoprotein

L-Glut	L-glutamine
$MgCl_2$	Magnesium chloride
MTT	Methylthiazol Tetrazolium
Na_2EDTA	Disodium ethylenediaminetetraacetic acid
NaCl	Sodium chloride
NAD	Nicotinamide adenine dinucleotide
NADPH	Nicotinamide adenine dinucleotide phosphate
NaOH	Sodium hydroxide
Nrf2	Nuclear factor-erythroid 2-related factor 2
NSAID	Non-steroidal anti-inflammatory drug
O^{2-}	Superoxide radical
OAT	Organic anion transporter
OGG1	8-oxoguanine glycosylase 1
-OH OTA	Hydroxy Ochratoxin A
OH^-	Hydroxyl radical
OP-OTA	Lactone opened Ochratoxin A
OTA	Ochratoxin A
OTB	Ochratoxin B
OTα	Ochratoxin α
PBS	Phosphate buffered saline
PEPCK	Phosphoenolpyruvate carboxykinase
PGC-1alpha	Peroxisome proliferator-activated receptor-gamma coactivator 1alpha
Phe	Phenylalanine
PKC	Protein kinase C
PSF	Penstrepfungizone

pSIRT1	Phospho-SIRT1
PUFA	Polyunsaturated fatty acid
qPCR	Quantitative polymerase chain reaction
RBI	Relative band intensity
RNA	Ribonucleic acid
ROS	Reactive oxygen species
RT	Room temperature
SA	South Africa
SCGE	Single cell gel electrophoresis
SDS	Sodium dodecyl sulphate
SDS-PAGE	Sodium dodecyl sulphate polyacrylamide gel electrophoresis
Sir2	Silent information regulator 2
SIRT1	Sirtuin 1
SOD	Superoxide dismutase
ssDNA	Single stranded DNA
TCEP	Tris (2-carboxyethyl) phosphine
TTBS	Tris-buffered saline and Tween 20
Tyr	Tyrosine
USA	United States of America
UTT	Urinary tract tumour
UV	Ultraviolet
γ-GCS	Gamma glutamylcysteine synthetase

List of Figures

Chapter 1

Figure 1	Structure of Ochratoxin A [1].	1
Figure 2	Map of the Balkan Peninsula.	2
Figure 3	Production of hydroxyl radicals by the Fenton reaction [2].	3
Figure 4	ROS affects DNA, lipids and proteins, contributing to dysfunctional cellular processes and aging (by author).	4
Figure 5	The effects of increased intracellular calcium as a mechanism of OTA toxicity (by author).	6
Figure 6	Toxicity of the OTA phenylalanine moiety (by author).	7
Figure 7	Biotransformation of OTA into various metabolites for detoxification (Adapted by author from Ringot *et al*., (2006)).	10
Figure 8	Image of *Botrytis cinerea* infection on grapes commonly used for wine production.	12
Figure 9	Structure of resveratrol [3].	13
Figure 10	Chemopreventive effects of resveratrol (by author).	16
Figure 11	Schematic diagram of the Nrf2-ARE pathway and its regulation by ROS (by author).	19

Chapter 2

Figure 12	MTT is reduced to a formazan product by viable cells, via a reaction catalysed by mitochondrial reductase (by author).	24
Figure 13	Diagram of a haemocytometer chamber used to calculate cell number and viability (Sigma Aldrich, BioFiles).	25
Figure 14	The GSH system of detoxification (by author).	26
Figure 15	Principle of the GSH luminometry assay (by author).	27
Figure 16	Representation of one cycle of the PCR target DNA amplification process (by author).	31
Figure 17	The reaction observed in the BCA assay during protein quantification (by author).	34
Figure 18	Colour changes seen in the BCA assay (by author).	35
Figure 19	Components of the transfer system (by author).	37
Figure 20	Chemiluminescent detection of the antibody-antigen reaction (by author).	38
Figure 21	Flow cytometer components [4].	39

Chapter 3

Figure 22 Percentage viability of cells exposed to OTA over 24 hours. An IC_{50} of 1.5µM was calculated from the dose-response curve. 41

Figure 23 Resveratrol significantly decreased the percentage of intracellular ROS (***p<0.0001), while OTA and OTA+Resveratrol treatments decreased the values of ROS when compared to control cells (*p=0.0048). 42

Figure 24 Assessment of DNA damage showing images of A) comet tails and B) the measurement of comet tail lengths. OTA increased comet tail lengths (***p<0.0001), while resveratrol significantly decreased lengths (***p<0.0001). C) The fold change analysis of OGG1 mRNA expression in cells exposed to OTA and resveratrol indicates that OTA significantly increased, while resveratrol significantly decreased expression of OGG1 mRNA (p<0.05). OTA+Resveratrol increased OGG1 mRNA expression. OTA+Resveratrol co-treated cells showed a significant increase in OGG1 mRNA expression when compared to OTA-exposed cells, which correlates to the events seen in the comet assay. 43

Figure 25 Concentrations of GSH and GSSG in HEK293 cells after exposure to OTA and resveratrol. The OTA+Resveratrol co-treatment increased the concentrations of GSH and GSSG (**p=0.0117), while resveratrol decreased GSH concentrations. 44

Figure 26 OTA, resveratrol and OTA+Resveratrol significantly increased the mRNA expression of genes associated with the antioxidant response in HEK293 cells – A) Nrf2 (*p<0.05), B) GPx (*p<0.05), C) CAT (*p<0.05) and D) SOD (*p<0.05). 46

Figure 27 Western blot images and relative fold change in protein levels of Nrf2 and pSIRT1 in response to OTA and resveratrol exposure. Resveratrol and OTA+Resveratrol significantly decreased the expression of Nrf2 (**p<0.05). Resveratrol and OTA+Resveratrol significantly increased the levels of pSIRT1 (***p=0.0002 and **p<0.05 respectively), indicating increased activation of SIRT1. 47

List of Tables

Table 1 List of primer sequences used for qPCR. 33

Table of Contents

Abstract	ii
Declaration	iv
Acknowledgements	v
Publications	vii
Presentations	viii
List of abbreviations	ix
List of figures	xiii
List of tables	xvii
Introduction	xxi
Aims and Objectives	xxiii
Chapter 1: Literature Review	**1**
1.1 Ochratoxin A: The Mysterious Mycotoxin	1
- 1.1.1 Toxicity of OTA	2
- 1.1.1.1 Oxidative stress induction by OTA	3
- 1.1.1.2 Genotoxicity of OTA	4
- 1.1.1.3 Calcium homeostasis disruptions	5
- 1.1.1.4 Protein synthesis disruptions	6
- 1.1.2 Exposure, Absorption and Distribution	7
- 1.1.3 Biotransformation and Elimination	9
1.2 Resveratrol: Therapeutic Potential	11
- 1.2.1 Description and Distribution	12
- 1.2.2 Bioavailability and Metabolism	13
- 1.2.3 Antioxidant effects	14

- 1.2.4 Anti-inflammatory properties 14

- 1.2.5 Chemopreventive potential 14

- 1.2.6 Cardiovascular protection 15

- 1.2.7 Resveratrol, Sirtuin 1 and Aging 17

1.3 Cytoprotective response 17

- 1.3.1 The Nuclear factor-erythroid 2-related factor 2 - Antioxidant Response Element (Nrf2-ARE) Dynamic 18

- 1.3.2 The antioxidant defence system 19

- 1.3.3 DNA damage and repair 21

Chapter 2: Materials and Methods 22

2.1 Materials 22

2.2 Cell culture 23

2.3 OTA treatments 23

2.4 MTT assay 23

2.5 Resveratrol treatments 24

2.6 Cell preparation for assays 25

2.7 Glutathione (GSH) and Glutathione Disulfide (GSSG) assay 26

2.8 Comet assay 28

2.9 Quantitative polymerase chain reaction 29

- 2.9.1 RNA extraction 31

- 2.9.2 cDNA Synthesis 32

- 2.9.3 qPCR 32

2.10 SDS-PAGE and Western Blotting 34

- 2.10.1 Protein isolation and sample preparation 34

- 2.10.2 SDS-Polyacrylamide gel electrophoresis (SDS-PAGE) and Transfer 36

- 2.10.3 Western blotting 37

2.11 Flow cytometry 39

2.12 Statistical analysis 40

Chapter 3: Results **41**

3.1 MTT assay 41

3.2 Analysis of intracellular ROS 41

3.3 Assessment of DNA damage and repair 42

3.4 Measurement of GSH and GSSG concentrations 44

3.5 qPCR analysis of antioxidant response 45

3.6 Western blotting 46

Chapter 4: Discussion **48**

Chapter 5: Conclusion **51**

References **52**

Appendix A **63**

Appendix B **64**

Appendix C **65**

Appendix D **66**

Introduction

Ochratoxin A (OTA) is a common contaminant of foods, such as grains, fruit and animal feed [5]. It is ubiquitously produced by fungal species of *Aspergillus* and *Penicillium*, specifically *Aspergillus ochraceus* [6]. Rural populations in developing countries rely heavily on grains as a staple source of sustenance; many of these communities lack proper storage facilities for harvested grains; this leads to increased fungal contamination and subsequent production of OTA [7]. Ochratoxin A was first discovered in South Africa (SA) in 1965 [8] and has since been found in food sources around the world [9]. Although first discovered in SA, there is still little documented information on OTA mycotoxicosis in SA. Understanding the mechanism of OTA toxicity is particularly important for African countries since grains, such as cassava and maize, contribute to a large part of the daily sustenance for a high percentage of the population [9].

Microorganisms in the gastrointestinal tract (GIT) hydrolyse OTA to the less toxic by-product, Ochratoxin α (OTα) [10], which is then excreted via the liver and kidney [11]. Exposure to high levels of OTA has also been linked to renal dysfunction and tumourigenesis in humans [12]. OTA is nephrotoxic and results in destruction of the renal tubular epithelium causing progressive renal failure [1]. This disease is particularly prominent in the Balkan regions such as Bulgaria and Romania, and is known as Balkan Endemic Nephropathy (BEN) [1].

OTA exerts its toxic effects via a number of mechanisms, the most prominent method is by induction of oxidative stress, thereby increasing the production of reactive oxygen species (ROS) [13]. OTA alters the antioxidant potential of the cell, increasing the oxidative stress placed on the cell [14]. During oxidative stress nuclear factor-erythroid 2-related factor 2

(Nrf2) dissociates from its inhibitor, Kelch-like ECH-associated protein 1 (Keap-1), translocates into the nucleus and binds to the antioxidant response element (ARE) resulting in the transcription of proteins associated with the antioxidant defence system [15].

Resveratrol (3, 4', 5-trihydroxy-*trans*-stilbene) is a polyphenol found in the skin of injured grapes and some fruit, and is therefore commonly present in wine and grape juice [16]. Resveratrol is synthesised by plants as a defensive mechanism and is proposed to have antimicrobial, antioxidant, anti-carcinogenic and anti-inflammatory properties [16]. This compound is widely studied and holds great potential in disease treatment. It is also thought to promote cardiovascular health and longevity of cells, and is therefore encouraged as part of a healthy diet [17]. Resveratrol possesses free radical scavenging potential, contributing to its antioxidant capacity [18]. The phytoalexin is also known to activate Sirtuin 1 (SIRT1), an NAD^+-dependent deacetylase known for its ability to modulate transcription of proteins that augment the oxidative stress response as well as proteins that promote cell survival in times of stress [18, 19]. These attributes could contribute to the compound's chemo-preventive ability, as well as the ability to diminish cellular damage due to oxidative stress [17].

The mechanisms of OTA toxicity and the cellular antioxidant response are relatively unknown. We investigated the cytotoxic effects of OTA on HEK293 cells after acute exposure (24hr). Thereafter, we investigated the therapeutic effects of resveratrol in untreated and OTA-treated HEK293 cells. The results can be used as insight into the effects of OTA in human kidney cells, and resveratrol may have potential in reducing OTA toxicity

Aims and Objectives

Aim:

To determine the therapeutic effects of resveratrol in human embryonic kidney (HEK293) cells exposed to Ochratoxin A.

Objectives:

- Investigate the antioxidant response in HEK293 cells when exposed to OTA and resveratrol. The antioxidant response of the kidney cells will be observed by measuring certain markers associated with the antioxidant response, such as Nrf2, catalase, superoxide dismutase, glutathione peroxidase and glutathione. The mRNA and protein expression of these markers will be measured.
- Determine the effects of both OTA and resveratrol on the DNA of HEK293 cells. The genotoxic potential of OTA will be observed by measuring strand breaks in DNA. Thereafter, the therapeutic effects of resveratrol will be investigated by measuring biomarkers associated with DNA damage repair, such as OGG1.
- Investigate the extent of ROS induction in HEK293 cells. The oxidative stress percentage will be measured by flow cytometry.

Chapter 1

1. Literature Review

1.1 Ochratoxin A: The Mysterious Mycotoxin

Ochratoxin A (OTA) is a ubiquitous mycotoxin, produced by species of *Penicillium* and *Aspergillus* fungi, specifically *P. verrucosum* and *A. ochraceus.* This mycotoxin frequently contaminates food products, such as cereals, grains, coffee, some fruits and even pork products if contamination of animal feed occurs. This contamination occurs when foods are incorrectly stored and fungal growth infects the food [20-24]. OTA is a chlorinated isocoumarin compound, which consists of a dihydroisocoumarin moiety linked to L-phenylalanine by a carboxyl group (Figure 1). Much controversy surrounds this mycotoxin, as an exact mechanism to its toxicity or metabolic pathway has not yet been elucidated. Much data has been collected on OTA since its discovery in South Africa in 1965, however a clear mechanism of action has not yet been found [8]. There are many proposed mechanisms of toxicity, and these could all contribute to the overall toxicity of OTA, which is known to be nephrotoxic and carcinogenic in rodents [20].

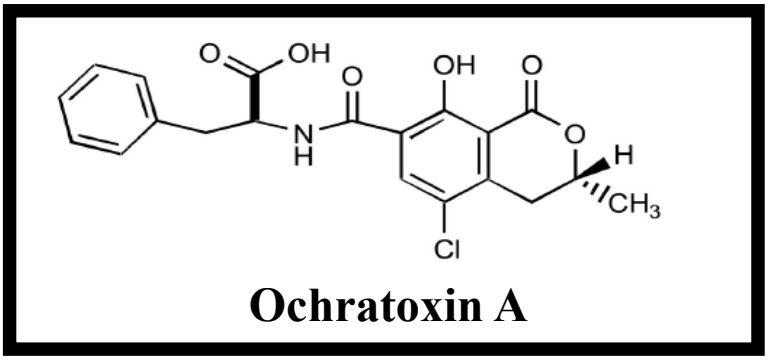

Figure 1: Structure of Ochratoxin A [1].

1.1.1 Toxicity of OTA

OTA exerts its toxic effects via a number of pathways, such as oxidative stress induction, protein synthesis inhibition, signal transduction disruptions and metabolic disturbances. These mechanisms can eventually lead to renal failure and carcinogenesis [25]. This end point is common in populations from the Balkan Peninsula (Figure 2), thus it has been termed Balkan Endemic Nephropathy (BEN). This disease is characterised by progressive renal failure, often occurring in individuals aged 30 to 40 years, occasionally accompanied by urinary tract tumours (UTT) [26]. Many studies have been conducted in this region of Europe involving consumer testing, which revealed OTA contamination in frequently consumed foods [13]. Thus, OTA has been linked as a causal factor in BEN. Subsequent testing using rodents has confirmed that OTA can induce UTT formation [27].

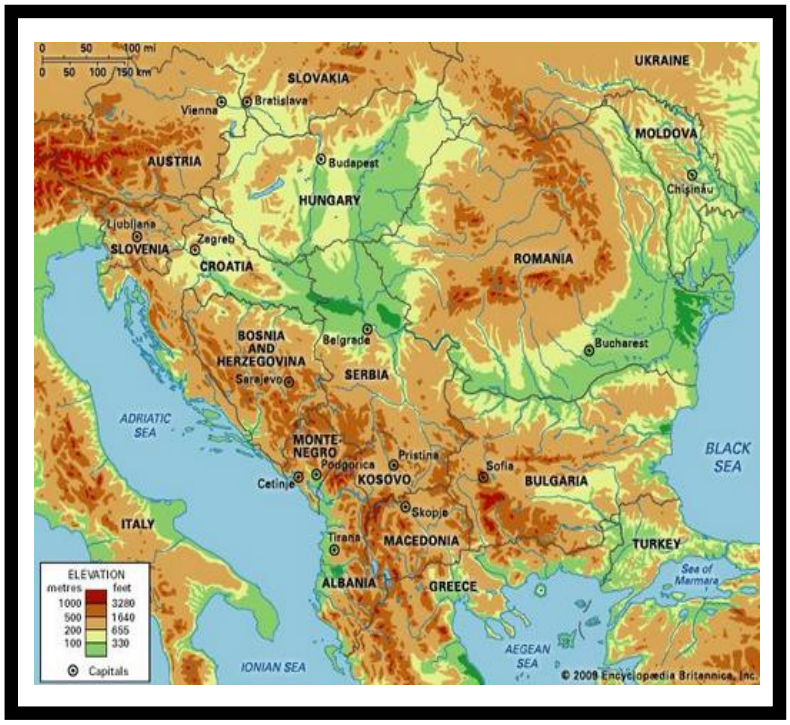

Figure 2: Map of the Balkan Peninsula [28].

1.1.1.1 Oxidative stress induction by OTA

Reactive oxygen species (ROS) formation occurs endogenously and is pivotal in normal cellular functions as well as during protective processes, such as the release of ROS from phagocytic cells to facilitate the destruction of infected or damaged cells. However, when ROS production outweighs the antioxidant capacity of the cell, cytotoxic situations arise [29].

The formation of ROS by OTA has been well documented, and this is often presented as the most feasible mechanism of toxicity. OTA is thought to disrupt the antioxidant defence response by inducing ROS formation at a rate too great for the cell to cope with [30]. OTA involvement in Fenton reactions has been documented; it is thought that the chlorine atom is involved in iron chelation, thus promoting the progression of Fenton reactions (Figure 3), fundamentally increasing the overall generation of ROS, with emphasis on hydroxyl radicals (OH^-) [31].

$$Fe\ (II) + H_2O_2 \rightarrow OH^- + OH + Fe\ (III)$$

Figure 3: Production of hydroxyl radicals by the Fenton reaction [2].

It has also been frequently reported that OTA down-regulates proteins associated with antioxidant defence systems, thus rendering the cell vulnerable to ROS-mediated attack. ROS can modify the behaviour of a cell and hence influence its survival (Figure 4) [1, 6, 32].

Mitochondrial functioning is affected by OTA, this could promote the release of electrons from the electron transport chain (ETC), contributing to the formation of superoxides [33]. Superoxides (O_2^-) are a form of free radicals, as are hydrogen peroxides (H_2O_2) and OH^-. The

hydroxyl radical is very reactive with biological molecules, such as lipids, proteins and DNA [2]. DNA strand breakage and disruptions in calcium (Ca^{2+}) homeostasis are early events of ROS-mediated damage.

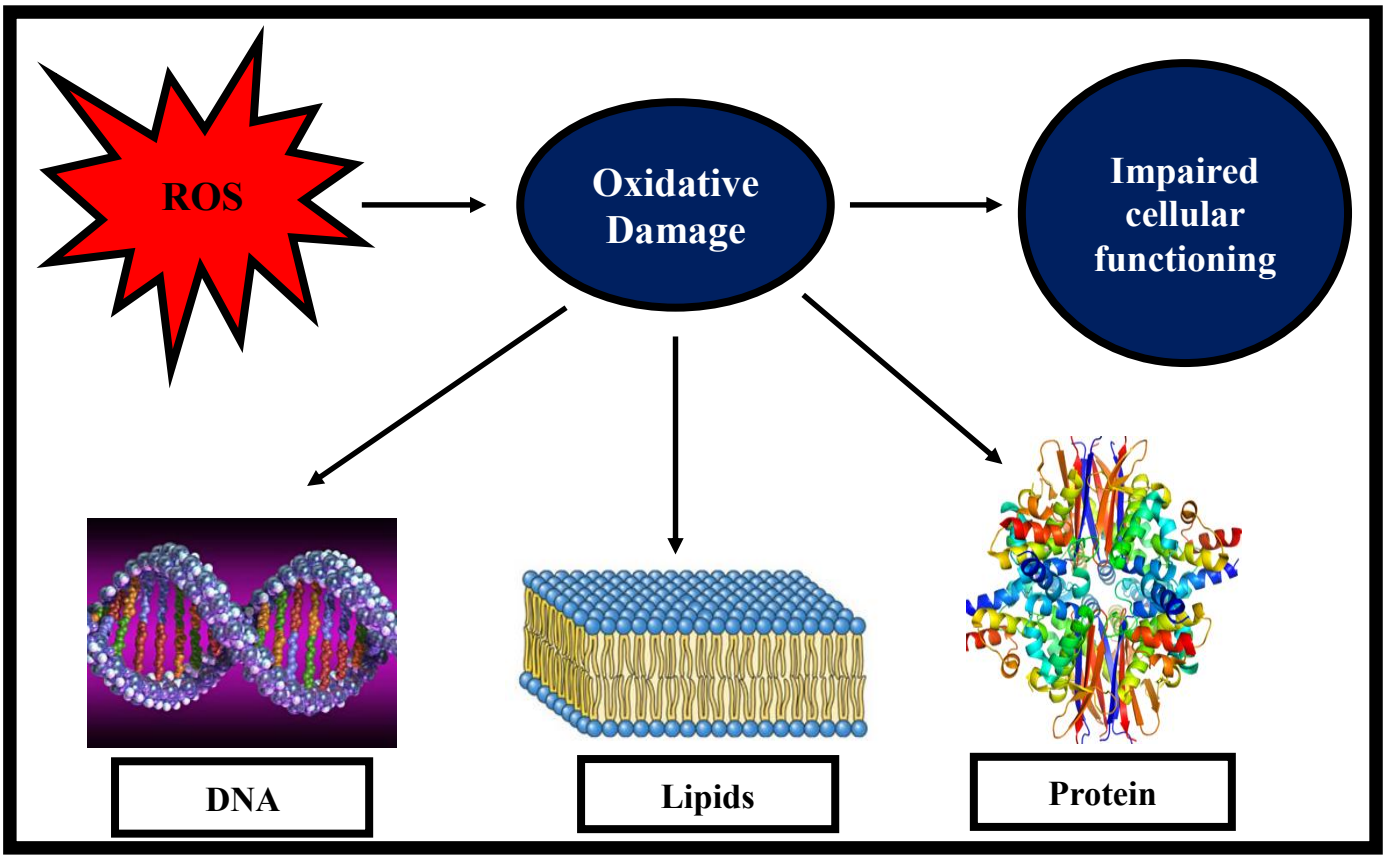

Figure 4: ROS affects DNA, lipids and proteins, contributing to dysfunctional cellular processes and aging.

1.1.1.2 Genotoxicity of OTA

Some authors state that OTA is directly genotoxic, and others believe that the toxin indirectly induces DNA damage by increasing ROS production. OTA can induce DNA strand breaks by increasing the formation of ROS, while simultaneously diminishing the antioxidant defence of the cell, which would allow free radicals to interact with DNA [34]. DNA strand breakage occurs when the highly reactive OH^- radical inserts itself into double bonds of DNA bases or

when it abstracts hydrogen (H^+) atoms from methyl groups of the base thymine [33]. The addition of OH^- into double bonds yields adduct radicals, while H^+ abstraction yields allyl radicals. These radicals then undergo a number of reactions, ultimately resulting in multiple DNA products; if the antioxidant response is not functioning optimally then this array of DNA bases would persist and eventually alter the structure and functioning of the genome, resulting in mutations [33]. DNA damage is a crucial event in the initiation of carcinogenesis. Many studies report that OTA always induces DNA fragmentation, however, it is unknown whether the toxin achieves this directly or indirectly. It is thought that OTA-mediated ROS induction and oxidative damage could contribute to the toxicity and carcinogenicity of OTA [34].

1.1.1.3 Calcium homeostasis disruptions

The second early event of ROS-induced damage is altered Ca^{2+} homeostasis. Calcium is an important second messenger and is responsible for the transfer of biological information. It is paramount in maintaining the proper functioning of cells, however, if not strictly regulated, fluctuations in Ca^{2+} homeostasis could be detrimental and possibly fatal to the cell [35]. OTA plays a role in the disruption of Ca^{2+} homeostasis, possibly contributing to its toxicity (Figure 5). The cell experiences increased calcium influx as well as increased release of calcium from stores, such as the endoplasmic reticulum (ER). Calcium sensitive channels are affected during this disrupted homeostasis, therefore OTA has the potential to disrupt all cellular functions that are calcium-dependent [32]. OTA promotes lipid peroxidation via increased ROS production; lipid peroxidation compromises the plasma membrane structure, thereby altering its permeability to Ca^{2+} ions, this in turn compromises Ca^{2+} homeostasis [32]. The OH^- radical exerts its effect on lipids by abstracting H^+ from polyunsaturated fatty acids (PUFAs) and thereby setting off a chain reaction, resulting in the mass formation of free radicals. This process results in lipid peroxidation, which is a late event of ROS-induced cell death [2].

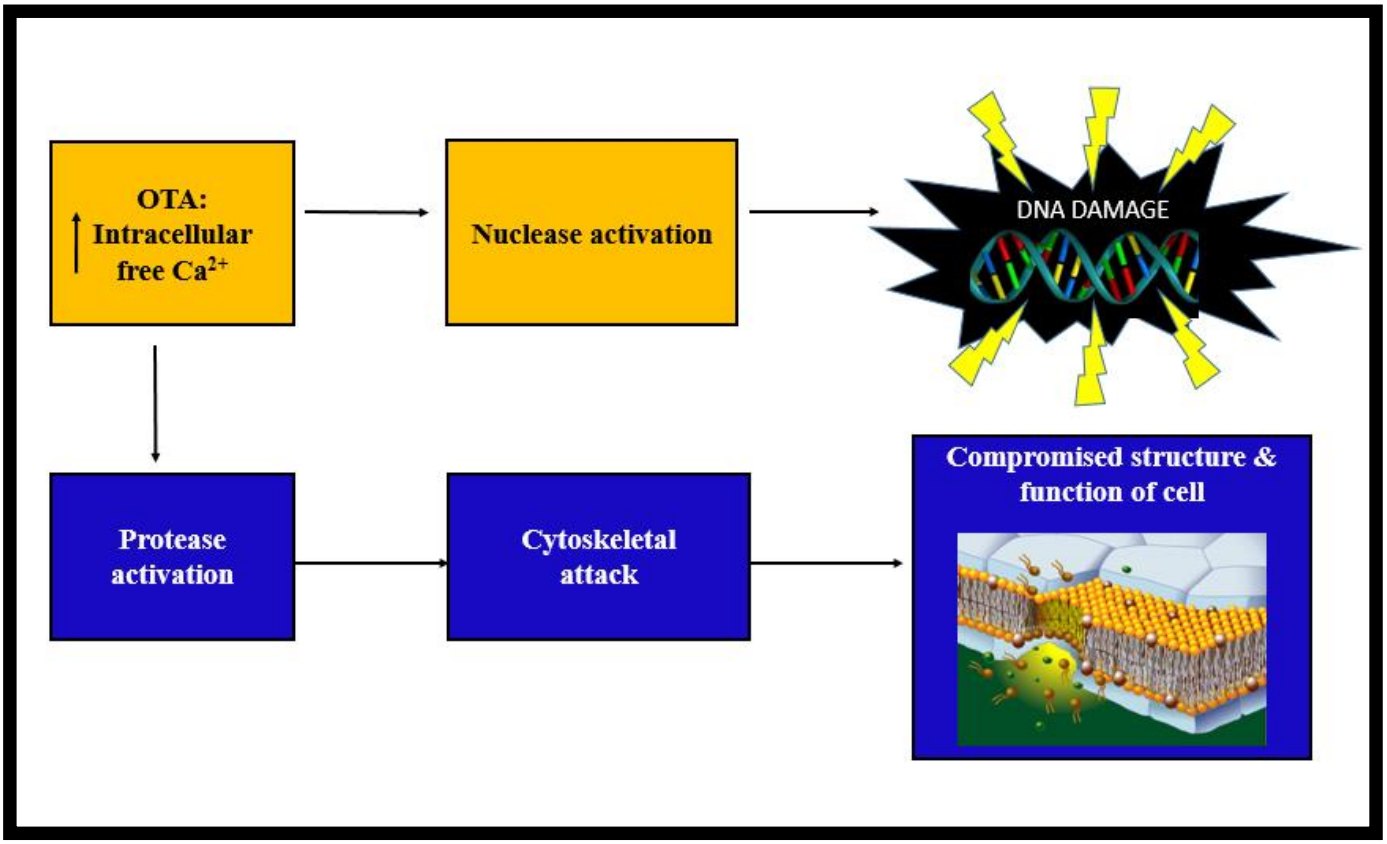

Figure 5: The effects of increased intracellular calcium as a mechanism of OTA toxicity.

1.1.1.4 Protein synthesis disruptions

The structure of OTA plays a crucial role in its mechanisms of toxicity. This mycotoxin possesses a phenylalanine (Phe) moiety, therefore allowing it to behave as a structural analogue to Phe [32]. OTA is able to mimic the amino acid and act on the systems that Phe is naturally involved in; it is by this method that OTA affects protein synthesis, Phe metabolism and, subsequently, enzyme production (Figure 6). Protein synthesis is affected by competitive inhibition of the enzyme phenylalanine-tyrosine (Phe-Tyr) synthase, the toxin inhibits Phe participation in this reaction by competing for the enzyme, in this manner peptide elongation as well as amino acylation is halted [36, 37]. Phe metabolism is disrupted by the interaction of OTA with Phe-hydroxylase; this enzyme is responsible for the conversion of Phe to Tyr during an irreversible hydroxylation reaction, which is an important step of Phe catabolism [37].

A mechanism of OTA toxicity could be the inhibition of Phe-hydroxylase or participation as a substrate for the enzyme, in place of Phe, by binding to specific activation sites on the enzyme and impairing the normal reaction. In this way OTA competes against Phe for its enzyme. The catabolism of Phe is tightly regulated to prevent the depletion or accumulation of Phe to unnatural levels, which could lead to decreased production of Phe requiring compounds. The involvement of OTA in this metabolic pathway could lead to phenylketonuria [32]. As a consequence to protein synthesis inhibition, enzyme synthesis is impaired, particularly affecting phosphoenolpyruvate carboxykinase (PEPCK). This is a fundamental enzyme in the gluconeogenic pathway, indicating that OTA indirectly affects carbohydrate metabolism [32].

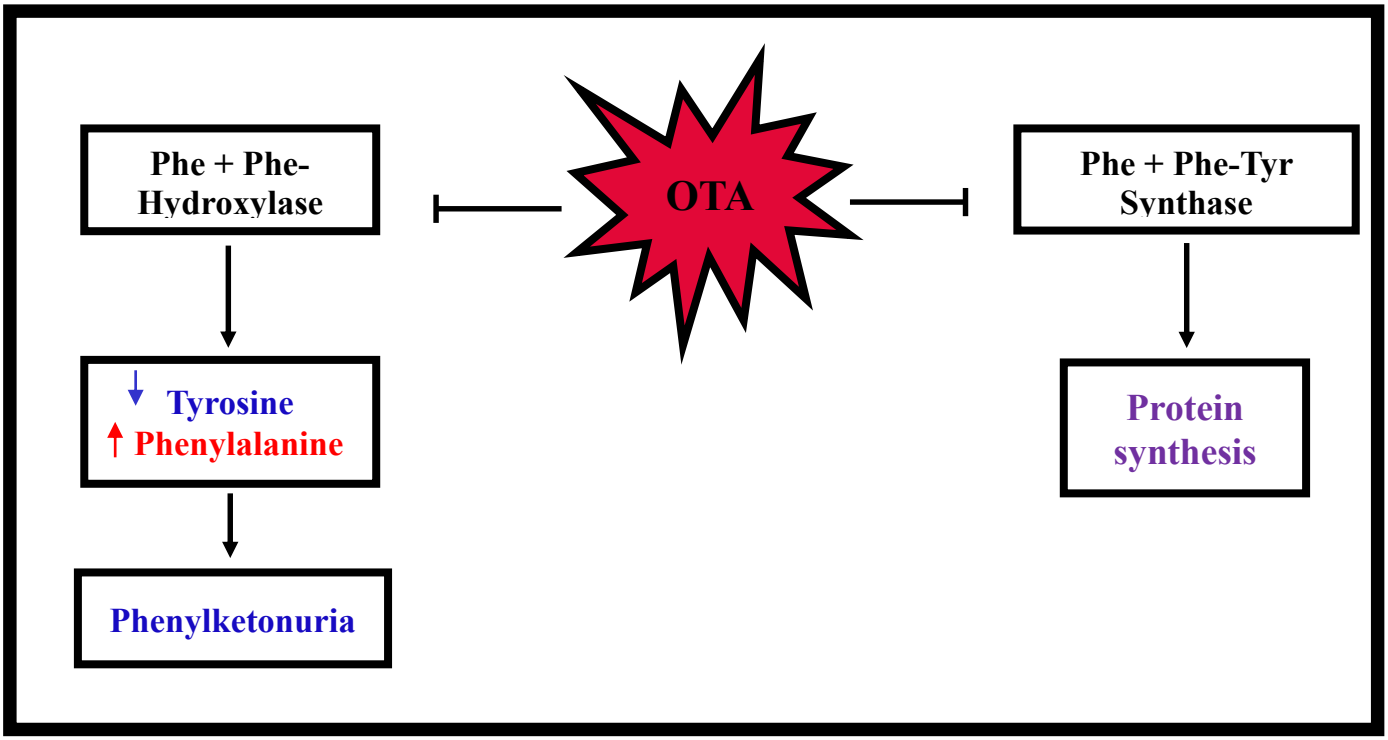

Figure 6: Toxicity of the OTA phenylalanine moiety.

1.1.2 Exposure, Absorption and Distribution

OTA exposure occurs via ingestion of contaminated food, such as grains, fruit, coffee beans, wines and animal products. *Aspergillus* and *Penicillium* fungi are responsible for the

production of OTA as a secondary metabolite during fungal contamination of foods. The toxicokinetics of OTA are difficult to follow since the toxin is involved in many reactions *in vivo*. Once OTA is ingested it is present in the mono-anion and di-anion forms in the duodenum due to the pH of chyme, it can then be passively absorbed in its non-ionised and mono-anion form. It can be readily absorbed from the small intestine into the blood where it becomes 99% bound to serum proteins, especially albumin [34]. The serum half-life in humans is the longest recorded half-life of OTA (35 days), however variations in the half-life exists depending on the degree of binding or the protein binding affinity. When OTA is protein-bound it becomes more difficult to eliminate, passive absorption is facilitated and as a result the half-life can become extended *in vivo* [1]. Albumin binding prevents toxin transfer from the blood to renal or hepatic cells, thus preventing its biotransformation for excretion purposes.

The concentration of OTA and its metabolites *in vivo* depend on a number of factors, namely animal species, the dose and forms of administered OTA, the diet composition and health status of the animal. Once OTA has been absorbed into the blood stream, it is transported to the kidney and other tissues [1]. In the kidney, specific organic anion transporters (OAT) facilitate cellular uptake. Since the toxin is protein-bound it can be absorbed at the proximal and distal tubules of the kidney, resulting in toxin accumulation in the kidney [32]. OTA has also been detected in human milk, which poses a considerable health risk to breast-feeding infants [9]. Kumagai *et al*. (1982) and Roth *et al* (1988) provided evidence that OTA participates in enterohepatic recycling. These studies have shown that a secondary OTA distribution peak was observed in the serum and intestine of rodents, which could be due to the process of enterohepatic recycling [38, 39].

1.1.3 Biotransformation & Elimination

Areas of high biotransformation, such as the liver and kidney, possess the potential to transform OTA into less toxic compounds using Phase I biotransformation reactions [40]. OTA is excreted via biliary (faeces) and renal (urine) routes, thus it interacts closely with the liver and kidney, which places these organs in a high risk situation, as OTA could easily exert toxic effects on hepatic and renal cells. Since OTA has a high affinity for plasma proteins, it is difficult to excrete the parent compound via glomerular filtration [1]. The toxin can also be reabsorbed at all nephron segments inducing an accumulation effect in the kidney and decreasing elimination. The highest concentrations of OTA can be found in the renal papilla and the medulla as a direct consequence of tubular reabsorption [32]. Biotransformation of the parent compound occurs to combat the persistence of OTA. OTA undergoes a number of reactions, yielding a variety of metabolic derivatives, each with its own set of characteristics and levels of toxicity (Figure 7).

Hydrolysis of the parent molecule occurs in the large intestine in the presence of microorganism-rich digesta [41]. OTA is converted to Ochratoxin α (OTα) when the peptide bond is cleaved by proteases, liberating the Phe moiety from the chlorinated dihydroisocoumarin moiety. It is thought that the microorganisms in the gut are responsible for this reaction; this information was used to conclude that ruminants enjoy an increased resistance to the toxic effects of OTA since the rumen of these animals contains higher levels of microorganisms, elevating the degradation of OTA to compounds that can be easily eliminated [10]. It has been proposed by Hohler *et al* (1999) that ruminants could be used to remove OTA from the food chain by feeding contaminated food to the animals, and allowing them to degrade the toxin [10]. Phase I reactions produce hydroxylated derivatives of OTA, namely 4(R)-OH OTA, 4(S)-OH OTA, 10-OH OTA, this can be achieved by the incubation of

OTA with liver and kidney microsomes. A small amount of the parent compound is converted to these hydroxylated derivatives by cytochrome P_{450} isoforms (*CYP_{450} 1A1/1A2/2B1/3A1/3A2*). The hydroxylated derivatives are less toxic than the parent compound and facilitate easier elimination [32].

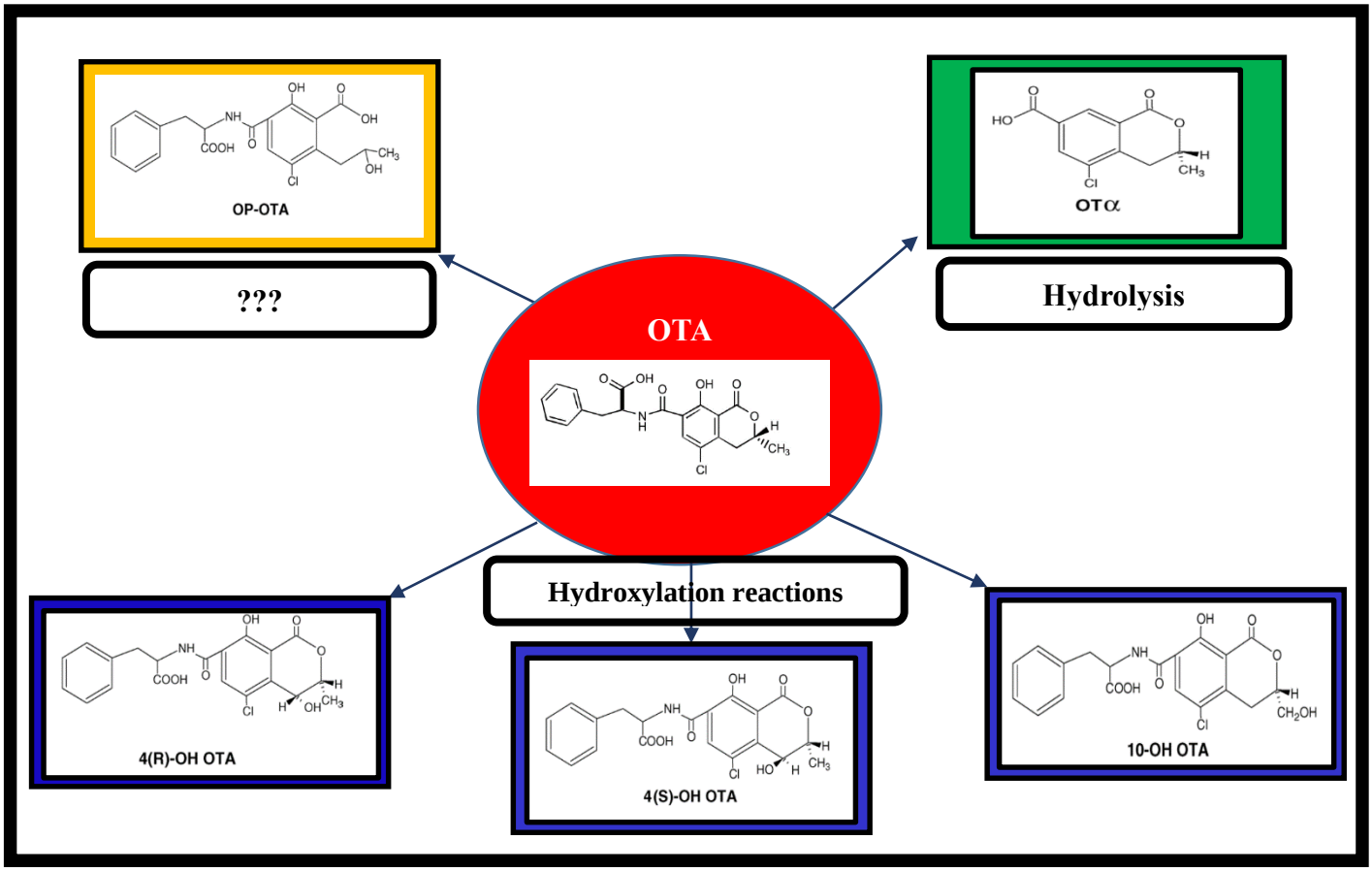

Figure 7: Biotransformation of OTA into various metabolites for detoxification (Adapted by author from Ringot *et al*., (2006)).

Ochratoxin B (OTB) is a dechloro-derivative of OTA and is far less toxic, possibly due to the lack of a chlorine atom, which decreases the ability of the toxin to chelate iron and thus decreases participation in Fenton reactions [32]. In the case of OTα, the phenylalanine moiety is removed, therefore decreasing the inhibition of protein synthesis and metabolic disturbances associated with the phenylalanine moiety in OTA. The metabolites produced from OTA

biotransformation is not always beneficial. The parent molecule could form a lactone-opened OTA (OP-OTA), as seen by Xiao *et al* (1996). The formation of this derivative is not clearly understood, however, it has been found to undergo clearance at a far slower rate that OTA and it appears to be extremely toxic in rats [42].

The kidney has been identified as the target organ of OTA, thus it experiences the brunt of OTA toxicity. The kidney attempts to eliminate OTA by excreting the parent compound or its derivatives in urine. However, during this process some reabsorption occurs, glomerular filtration is limited and OTA accumulates in the kidney, thus increasing the toxin's contact time with renal cells. Heussner *et al*. (2007) suggested that repeated exposure of renal epithelium to OTA altered the normal structure and functioning of the tissue. This research indicated that renal epithelium experienced a conversion to a more fibroblast-like nature, as fibroblasts are less vulnerable to the effects of OTA [43]. During this conversion the cell increases collagen production. OTA exposure induces renal cell death, and the kidney attempts to compensate for this cell death by augmenting the repair and regenerative processes. This process involves the migration and proliferation of renal cells, during proliferation the cells undergo differentiation, which alters the cell type and steers it towards fibroblast characteristics [43]. These changes in renal cells result in progressive fibrosis, which is a late stage event seen in BEN. OTA-induced nephrotoxicity can be recognised by glucosuria, proteinuria and renal dysfunction, which can be confirmed by observing increased urea and creatinine levels in the blood as well as decreased glucose and protein in the serum.

1.2 Resveratrol: Therapeutic Potential

Resveratrol is a phytoalexin frequently produced by plants in response to cellular damage or fungal infection. This compound is commonly found in the skins of grapes, *Vitis vinifera*, as a

response to ultraviolet (UV) damage or infection with *Botrytis cinerea* [16]. The phytoalexin is known to have a vast array of health benefits and dates back to its use in Chinese and Japanese traditional medicine [19]. The compound was first isolated in 1940 by Michio Takaoka from the roots of white hellebore, a flowering plant belonging to the family *Ranunculaceae* [44, 45]. Further derivatives of this trans-hydroxystilbene was discovered in subsequent years.

Figure 8: Image of *Botrytis cinerea* infection on grapes commonly used for wine production.

1.2.1 Description & Distribution

Trans-resveratrol was first discovered in the skins of grapes in 1976 by Langcake and Pryce [46]. It has since been studied and synthesised organically; the compound can remain stable for many months if protected from light [47]. Resveratrol is commonly found in wines and grape juice as a result of the compounds presence in grape skins, it can also be found in berries, peanuts and other plant sources. One gram of grape skin can contain anywhere from 50µg to 100µg resveratrol [16].

The concentration of resveratrol present in wines depends on a number of factors; namely, the type of grape, the geographic region of grape growth, the severity of *Botrytis* infection, the type of wine being produced (since maceration time influences the degree of grape skin injury) and

fermentation time (as it influences the contact of grape skin with the wine being produced) [47].

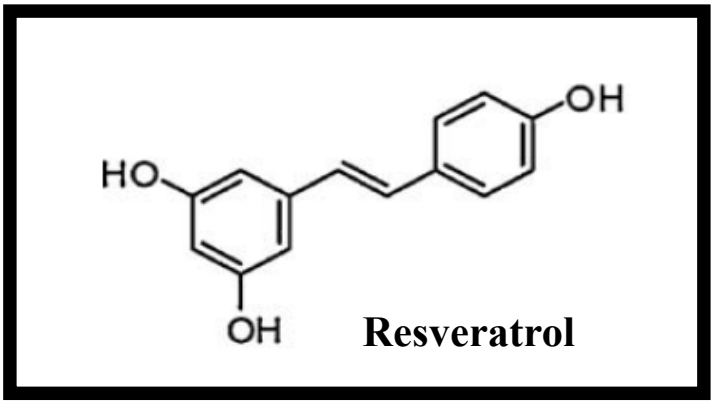

Figure 9: Structure of resveratrol [3].

1.2.2 Bioavailability and Metabolism

Resveratrol is frequently ingested with food products, it is easily absorbed from the GIT and rapidly metabolised in the liver by phase II biotransformation enzymes which render the compound soluble in water. Glycosylated resveratrol is said to be more stable and serves to protect the compound from oxidative degradation [16]. Resveratrol can possibly accumulate in epithelial cells along the aerodigestive tract; and these metabolites could contribute to the cardiovascular protective and chemopreventive properties of resveratrol.

Three main pathways are functional in the metabolism of resveratrol. This phytoalexin can undergo sulphate and glucuronic acid conjugation of phenolic groups, as well as hydrogenation of the aliphatic double bond, which is thought to be carried out by microflora residing in the intestine [48]. Sulphate and glucuronic acid conjugates have been found in the urine. Trace amounts of unchanged resveratrol have been discovered in systemic circulation, while trans-resveratrol-3-O-glucuronide and trans-resveratrol-3-O-sulphate has been detected in the urine

[16]. The bioavailability and efficacy of resveratrol metabolites is unknown and further research needs to be conducted on this subject.

1.2.3 Antioxidant effects

Resveratrol has been proven to possess a multitude of antioxidant effects ranging from the ability to decrease lipid peroxidation, scavenge free radicals and chelate copper [47, 49-51]. Bradamante *et al*. (2004) reported that resveratrol scavenges hydroxyl and superoxide radicals. It also has the ability to scavenge metal-induced radicals, thus preventing lipid peroxidation and low-density lipoprotein (LDL) oxidation by diminishing the involvement of Fe^{2+} and Cu^{2+} in the respective reactions [52]. Resveratrol is known to exert protective effects over the kidney by modulating the expression of protective enzymes, such as glutathione peroxidase (GPx), superoxide dismutase (SOD) and catalase (CAT) through nuclear factor-erythroid 2-related factor 2 (Nrf2) -mediated regulation, resulting in decreased renal oxidative stress [53].

1.2.4 Anti-inflammatory properties

Resveratrol has been linked to anti-inflammatory abilities, similar to that of non-steroidal anti-inflammatory drugs (NSAIDs), whereby it inhibits cyclooxygenase (COX) activity, thus preventing COX-mediated arachidonic acid conversion to prostaglandins [54]. Decreased prostaglandin synthesis would contribute to decreased platelet aggregation and increased vasodilation that accompanies resveratrol exposure [55].

1.2.5 Chemopreventive potential

Taken together, the antioxidant and anti-inflammatory properties of resveratrol can contribute to chemoprevention [56-58]. As indicated by Jang *et al.* (1996), resveratrol is able to prevent

the three major stages of carcinogenesis, namely, initiation, promotion and progression. Firstly, the authors provided evidence that resveratrol prevents initiation by behaving as an antioxidant and antimutagen. The compound performs this feat by inducing phase II drug-metabolising enzymes, such as quinone reductase, which serves to detoxify carcinogens. Secondly, the anti-inflammatory effects result in the inhibition of COX-1, which prevents an inflammatory environment by decreasing the production of prostaglandins [17]. Prostaglandins are known to stimulate tumour growth as well as diminish immune system efficiency, while COX-1 participates in the activation of carcinogens to reactive intermediates that could induce DNA damage.

Resveratrol can also inhibit protein kinase C (PKC), which is responsible for COX activation. Therefore, resveratrol also serves to protect DNA from carcinogen attack. Thirdly, resveratrol has been recorded inducing differentiation, which would prevent tumour progression, in human promyelocytic leukaemia cells [54].

1.2.6 Cardiovascular protection

Resveratrol exerts protective effects on the cardiovascular system. Many authors refer to the "French Paradox" as a testament to the cardiovascular protective effects of resveratrol [50, 51]. This phenomenon illustrates that although the French people enjoy a diet high in saturated fats, the frequent consumption of red wine decreases death by coronary heart disease (CHD) [59]. An interest in red wine was piqued and resveratrol was discovered as the specific compound with cardiovascular health properties [60].

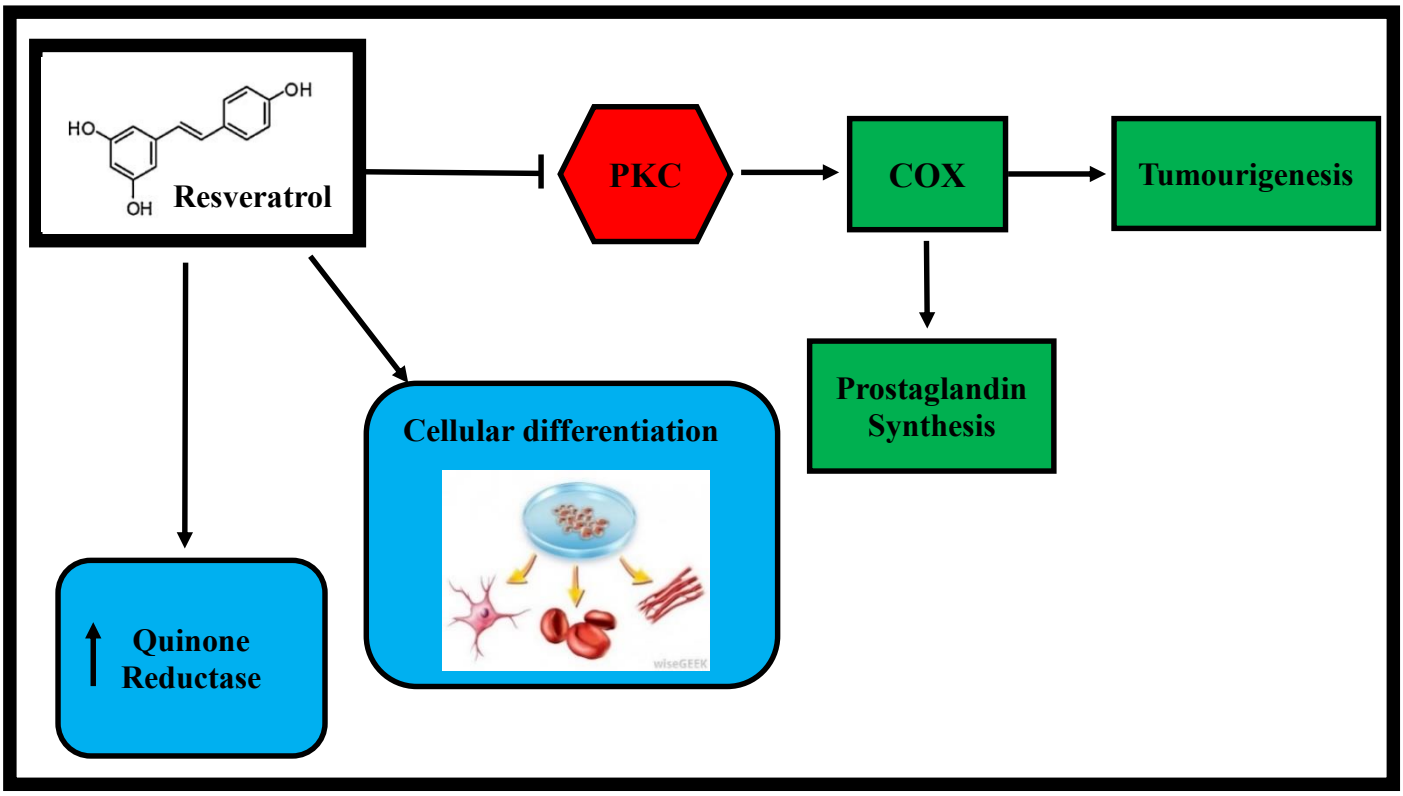

Figure 10: Chemopreventive effects of Resveratrol.

The antioxidant and anti-inflammatory characteristics of resveratrol also contribute to its cardiovascular protective properties. Reduction of free radicals, as a result of resveratrol-mediated free-radical scavenging, in turn decreases the extent of LDL oxidation, which ultimately contributes to CHD, since oxidised LDL can be found in atherosclerotic lesions [61, 62]. Resveratrol also serves to decrease serum lipid levels through an undefined mechanism. Platelet aggregation is diminished by resveratrol due to its apoptosis and thrombosis disrupting attributes [47, 63-66]. Resveratrol has the ability to inhibit thromboxane B2, a stable metabolite of thromboxane A2, thereby decreasing vasoconstriction. The COX pathways also mediate the state of vascular endothelium, governing vasoconstriction or vasodilation. In this manner, resveratrol serves to protect the cardiovascular system [52].

1.2.7 Resveratrol, Sirtuin 1 and Aging

The hallmarks of aging include decreased cellular responsiveness to stress, disruptions in cellular homeostasis and eventual organ dysfunction. Calorie restriction (CR) has been found to decrease the effects of aging, delay the onset of age-related diseases and extend lifespan [67]. The silent information regulator 2 (Sir2), found in *Saccharomyces cerevisiae* (yeast), has been identified as a molecule that participates in the process by which CR mediates cellular health and extends life [17, 68]. Sirtuin 1 (SIRT1) is an NAD^+-dependent deacetylase, which is a mammalian homologue to Sir2 and has been proven to function in a similar manner [69]. SIRT1 functions in metabolic and cellular stress response by altering certain cellular processes upon receiving stress signals. The main function of SIRT1 is to promote cell survival and confer resistance to stress-induced cytotoxicity. This deacetylase modulates cellular response to stress, in order to decrease oxidative damage and prevent replication of damaged DNA, thereby reducing the chance of mutation accumulation [53].

Calorie restriction has been found to increase SIRT1 expression, which in turn modifies the cell's response to stress and aging. SIRT1 exerts a protective effect by preventing DNA damage, mutations and genomic instability, as well as reducing oxidative stress and the damage it induces [3]. Resveratrol has been hailed as a "Sirtuin Activator" due to results from many tests conducted both *in vitro* and *in vivo*. Barger *et al.* (2008) shows that resveratrol can mimic the CR phenomenon and thereby induce SIRT1 activation and life extension [3, 70].

1.3 Cytoprotective response

The cell has many defence mechanisms and regulatory systems in place to defend against cellular damage and neutralise any threats that the cell might encounter. These cytoprotective responses are swift and function efficiently in a healthy cell.

1.3.1 The Nuclear factor-erythroid 2-related factor 2-Antioxidant Response Element (Nrf2-ARE) dynamic

Nuclear factor-erythroid 2-related factor 2 (Nrf2) is a transcription factor which is responsible for the activation of the antioxidant response element (ARE). This element regulates the transcription of enzymes during periods of cellular stress [71]. The ARE is a DNA element that is responsible for the coding of antioxidant enzymes, it is activated when stress signals induce the activation of Nrf2. Such signals include oxidative stress, decreased antioxidant capacity of the cell (GSH), the presence of chemicals capable of redox cycling and the biotransformation of xenobiotics into reactive intermediates.

In a resting cell, Nrf2 is retained in the cytoplasm by its inhibitor, Keap1 [15]. This transcription factor is very unstable and is thus degraded by proteases through ubiquitylation by Keap1. However, when stress signals are received, Nrf2 breaks its association with Keap1 in the cytoplasm and translocates to the nucleus, where it heterodimerizes with a small Maf protein, a protein thought to play a role as a transcriptional activator of Nrf2. This complex then binds to the ARE, inducing the activation of this element [72]. Activation of the ARE results in the transcription of genes associated with the antioxidant defence system (Figure11). These enzymes are produced in response to stress signals and attempt to remedy the situation to bring about cellular homeostasis.

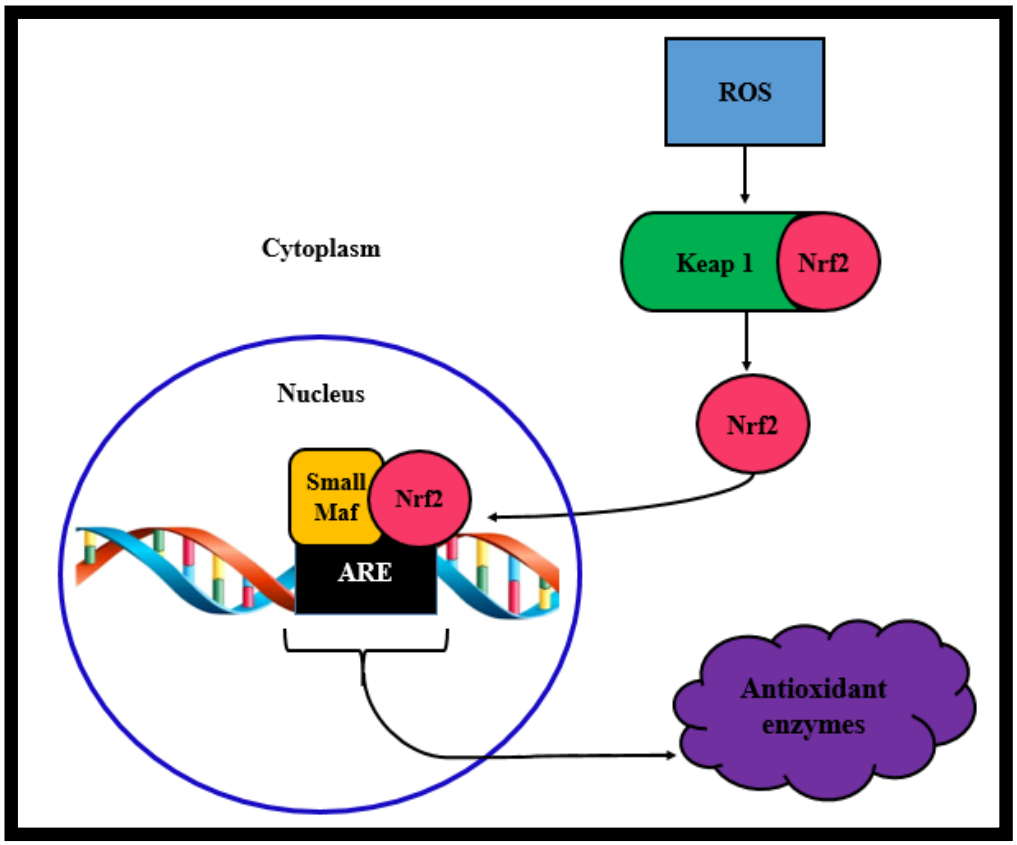

Figure 11: Schematic diagram of the Nrf2-ARE pathway and its regulation by ROS.

1.3.2 The antioxidant defence system

Antioxidant defence is initiated by the ARE upon activation by Nrf2. The interaction of Nrf2 and the ARE results in the production of a number of enzymes that serve to protect the cell from oxidative stress. Increased oxidative stress influences a number of processes and could conclude in cell death, mutations or carcinogenesis as a result of ROS interaction with biological molecules. The concentration of intracellular ROS depends on the rate of removal by the antioxidant system as well as the simultaneous rate of ROS production. Antioxidant enzymes, such as SOD, CAT and GPx, are necessary to maintain cellular health, since ROS is also produced endogenously and must be tightly regulated [73].

These enzymes function together for optimum detoxification of cellular stressors with emphasis on oxidative stress. Superoxide dismutase is found in intracellular cytoplasmic spaces and serves to degrade superoxide anions by catalysing their dismutation, resulting in the formation of hydrogen peroxide [73]. Catalase functions to reduce oxidative stress mediated cellular damage. This ubiquitous enzyme is a tetrameric protein with a heme group present in each subunit; it has earned the reputation of being the most efficient enzyme by binding and degrading up to 1 million H_2O_2 molecules per second. Catalase is a cytosolic selenoprotein, which serves to protect red blood cells from the oxidative degradation of haemoglobin by catalysing the reduction of H_2O_2 to water [74].

Overexpression of GPx results in increased protection against ROS-mediated assault. This enzyme requires several cofactors in order to function optimally; an especially important cofactor is the tripeptide thiol, Glutathione (GSH), which consists of γ-glutamate, cysteine and glycine [75]. GSH functions as an intracellular and extracellular antioxidant, it is an important ROS scavenger and its ratio with glutathione disulfide (GSSG) is a marker of oxidative stress. Synthesis of GSH is regulated by two enzymes, γ-glutamylcysteine synthetase (γ-GCS) and GSH synthetase, as well as by the concentration of cysteine, since this is a rate-limiting substrate for the *de novo* synthesis of GSH [76]. In turn, GSH regulates the formation of γ-GCS by negative feedback. The ratio of GSH:GSSG is influenced by GSH reductase, as well as the production of ROS and therefore, the activity of GPx. GSH reductase is a constantly active enzyme, which serves to promote the reduction of GSSG to GSH in order to allow maximal functioning of GPx [77]. Activity of GSH reductase increases upon increased oxidative stress. The GSH:GSSG ratio exists at a ratio of greater than 100:1 in a healthy, resting cell; however, during oxidative stress conditions, this ratio can decline to 10:1 and even 1:1 in

extreme cases [77]. These enzymes function to prevent ROS-induced damage in the cell, nonetheless, in times of excessive stress these measures fail and oxidative damage occurs.

1.3.3 DNA damage and Repair

It is known that oxidative stress can induce DNA strand breakage and eventually mutations, which could drive the cell towards cancer initiation [33]. In the event that antioxidant response systems fail and DNA damage occurs, the cell possesses multiple repair mechanisms to attempt to salvage the damaged DNA. One such example of this repair crew is 8-oxoguanine-DNA-glycosylase (OGG1), which functions to bring about DNA repair. This glycosylase enzyme belongs to a family of base excision repair (BER) proteins. It functions in the BER pathway by removing 8-oxoguanine base lesions, which are produced by ROS, via a glycolytic mechanism [33]. These lesions are highly mutagenic; they result from mispairs with adenine residues, causing a G:C to T:A transverse mutation [78].

In this manner, OGG1 plays a crucial role in the prevention of ROS-induced tumour formation. In the event that OGG1 becomes inactive, base lesions could accumulate, thereby increasing the likelihood of mutations and the possibility of carcinogenesis. Diminished DNA repair capacity is a marker for cancer susceptibility. Therefore, decreased functioning of fundamental repair enzymes would render the cell vulnerable to cancer initiation [33].

Chapter 2

2. Materials and Methods

2.1 Materials

All tissue culture consumables were purchased from Whitehead Scientific (Johannesburg, SA). The HEK293 cells were obtained from Highveld Biological (Johannesburg, SA). Ochratoxin A and resveratrol were purchased from Sigma Aldrich. Methylthiazoltetrazolium (MTT) salt, phosphate buffered saline (PBS) tablets and agarose were purchased from Capital Laboratory Supplies (Johannesburg, SA). The bicinchoninic acid (BCA) assay kit and tris-chloride were purchased from Sigma Aldrich (Johannesburg, SA). Kits and reagents used for luminometry (GSH-Glo™ Glutathione Assay kit) were purchased from Promega (United Sates of America (USA)).

Reagents for qPCR were purchased from Bio-Rad and the primer sequences were purchased from Inqaba Biotechnologies. Western Blotting reagents (Laemmli sample buffer and chemiluminescent reagents) were obtained from Bio-Rad (USA). Primary antibodies (rabbit anti-Nrf2 (8882) and rabbit anti-pSIRT1 (2314L)) were purchased from Cell Signalling (USA) and horse-radish peroxidase (HRP) – conjugated secondary antibodies (anti-rabbit IgG) were purchased from Santa Cruz Biotechnology (USA). Proteins were standardised to anti-β-actin (A3854) from Sigma Aldrich (USA). All other solvents and salts were purchased from Merck Chemicals (Johannesburg, SA). Protein isolation was conducted using Cytobuster^{TM} (Novagen) supplemented with protease inhibitors (Roche 05892791001) and phosphatase inhibitors (04906837001).

2.2 Cell culture

HEK293 cells were cultured in monolayer (10^6 cells per $25cm^3$ culture flask). The cells were maintained in complete culture medium (CCM: Dulbecco's Minimum Essential Media (DMEM), 10% foetal calf serum (FCS), 1% Penstrepfungizone (PSF) and 1% L-glutamine (L-Glut)) and incubated overnight at 37°C in a humidified incubator supplied with 5% CO_2. Cells were washed with 1.0M PBS. Once 80 % confluent, cells were removed using trypsin and agitating the flasks, cells were then counted using the Trypan Blue exclusion assay.

2.3 OTA treatments

A stock solution of 200µM OTA was prepared in 60% dimethyl sulphoxide (DMSO). Cells were treated with a range (0.25µM–50µM) of concentrations to obtain a half maximal inhibitory concentration (IC_{50}).

2.4 Methylthiazoltetrazolium (MTT) assay

The yellow MTT salt (3-(4,5-dimethylthiazol-2-yl)-2,5-diphenyltetrazolium bromide) is water soluble and thus forms a solution when dissolved in 1.0M PBS, which is converted to a water-insoluble, purple formazan ((2*E*,4*Z*)-(4,5-dimethylthiazol-2-yl)-3,5-diphenylformazan) by viable cells (Figure 12) [79]. The reaction is catalysed by mitochondrial reductase, and involves the reduction of MTT by reducing molecules, such as nicotinamide adenine dinucleotide (NADH). The MTT assay is a colorimetric assay used to determine cell viability by exploiting the conversion of MTT to formazan crystals by living cells, the intensity of the formazan product is proportional to the percentage of viable cells present [79].

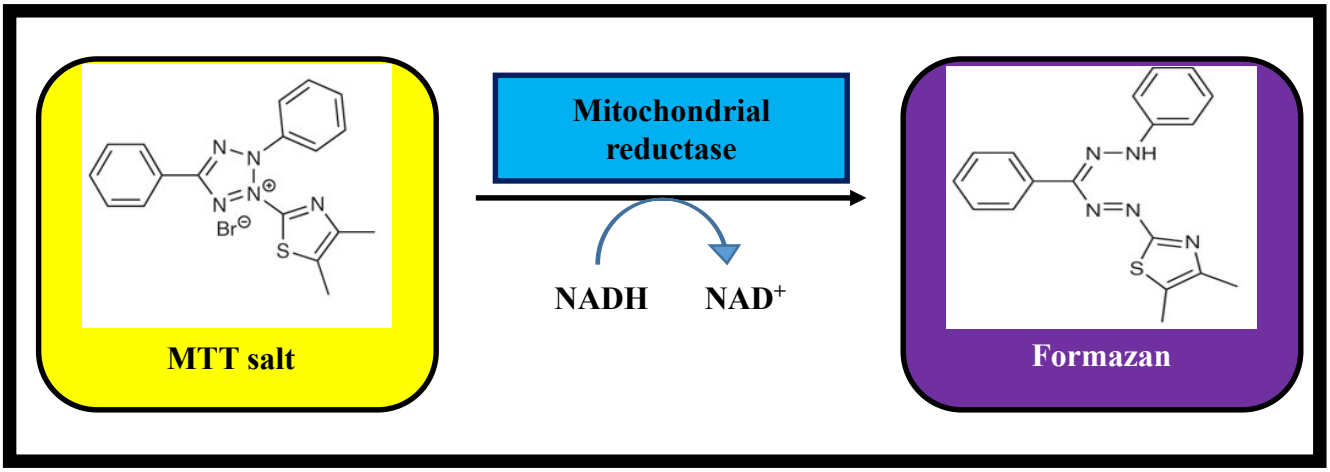

Figure 12: MTT is reduced to a formazan product by viable cells, via a reaction catalysed by mitochondrial reductase.

To determine cell viability cells were seeded into a 96-well microtitre plate (15,000 cells/well) and allowed to attach overnight. Attached cells were treated with a range of OTA concentrations (0.25µM–50µM) for 24hrs. Treatment media was removed and replaced with CCM (100µl) and 20µl MTT salt solution (5mg/ml in PBS). Cells were incubated with the MTT salt solution for 4hrs, then discarded and DMSO (100µl) was added; the cells were incubated with DMSO for 1hr. Absorbance was read using a Bio-Tek MQx200 spectrophotometer (SA) at 595nm (reference wavelength 655nm). An inhibitory concentration at which 50% of cell growth was inhibited (IC_{50}) was calculated using GraphPad Prism Statistical Software (version 5).

2.5 Resveratrol treatments

Stock solutions of 10mM resveratrol were prepared in 100% DMSO. Preliminary assays were carried out to determine the optimal resveratrol concentrations for all subsequent treatments. Cells were treated with 25µM, 50µM and 100µM resveratrol during pre-, post- and co-OTA treatments for 24hrs. The cells were then removed and counted according to the requirements

for each assay. Flow cytometry (10^6 cells/treatment) was used to observe which resveratrol concentration greatly decreased the percentage of intracellular ROS, while luminometry (10^4 cells/well) was used to detect the levels of intracellular GSH, thus indicating which concentration provided a more robust defence against oxidative damage. Based on these results, 25µM resveratrol was used for all subsequent assays.

2.6 Cell preparation for assays

Cells were treated once flasks reached confluency (10^6 cells/flask). Treatments included a control (CCM containing the solvent vehicle, DMSO), the IC_{50} value of OTA (1.5µM), a resveratrol control (CCM containing 25µM resveratrol) and a co-treatment (1.5µM OTA and 25µM resveratrol in CCM). Treatments were incubated over 24hrs. Cells were removed by trypsinisation and agitation, the Trypan Blue method of cell counting was employed to determine cell viability and number as required per assay performed (Figure 13). The control was used for statistical comparison to all other treatments.

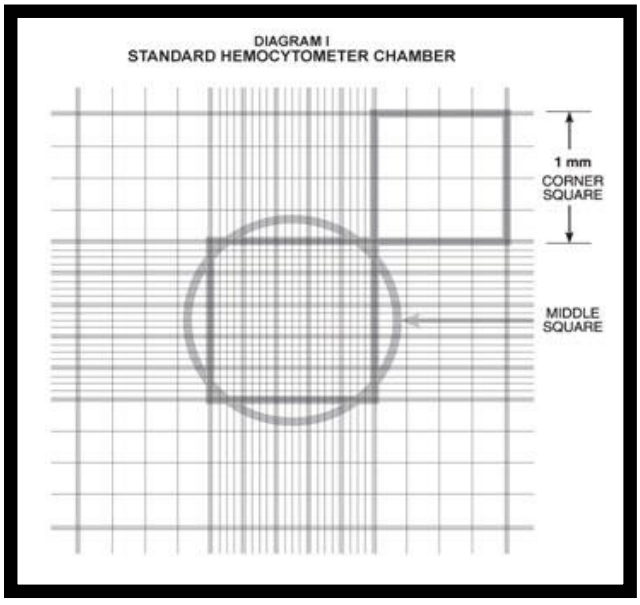

Figure 13: Diagram of a haemocytometer chamber used to calculate cell number and viability (Sigma Aldrich BioFiles).

2.7 Glutathione (GSH) and glutathione disulfide (GSSG) assay

Glutathione is a low molecular weight thiol consisting of three amino acids – cysteine, glycine and glutamine. GSH functions as a free radical scavenger by donating electrons (e^-) to free radicals, thereby detoxifying reactive species [80]. This free radical scavenger, which exists in reduced (GSH) or oxidised (GSSG) forms, is tightly regulated by a number of enzymes governing its production and functioning (Figure 14). GPx uses GSH as a cofactor to detoxify H_2O_2 to water, glutathione reductase (GR) manages the form of GSH present in the cell, and glucose-6-phosphate dehydrogenase (G6PD) maintains the level of nicotinamide adenine dinucleotide phosphate (NADPH), which maintains the level of GSH in cells [75].

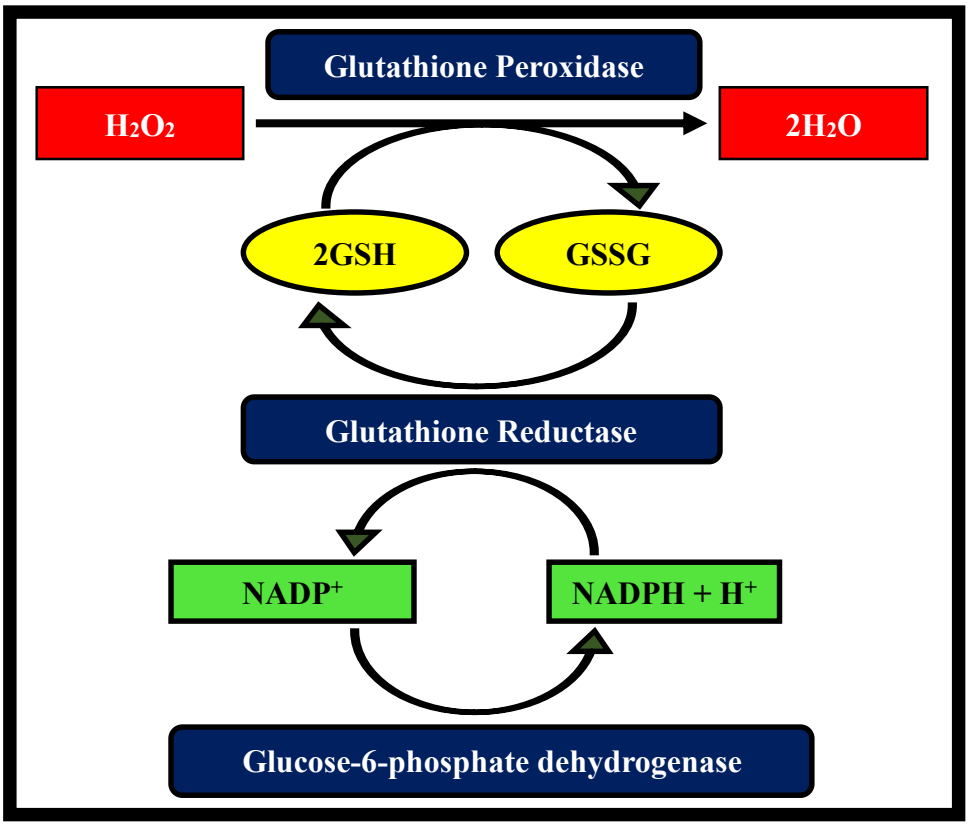

Figure 14: The GSH system of detoxification.

The GSH Assay (per GSH-Glo™ Glutathione Assay (Promega) protocol) was used to determine the concentration of GSH and oxidised GSH (GSSG) in HEK293 cells. Cells

(10^4cells/well) were seeded in a luminometry plate in 6 replicates. Standards (0-50µM) were added in triplicate to generate a standard curve of known GSH concentrations. Tris (2-carboxyethyl) phosphine (TCEP) was used as a reducing agent to reduce GSSG to GSH and thus measure the concentration of total GSH+GSSG in the cells. TCEP was added to cells in triplicate and agitated for 10sec, the GSH-Glo™ reagent (50µl) was added to each well; the plate was agitated for 30sec, and incubated in the dark (RT, 30min). The luciferin detection agent (100µl) was added to each sample and incubated as previously described (RT, 15min). The plates were read on a Modulus™ microplate luminometer (Turner Biosystems, Sunnyvale, USA). The GSH concentrations were determined by extrapolation from the standard curve.

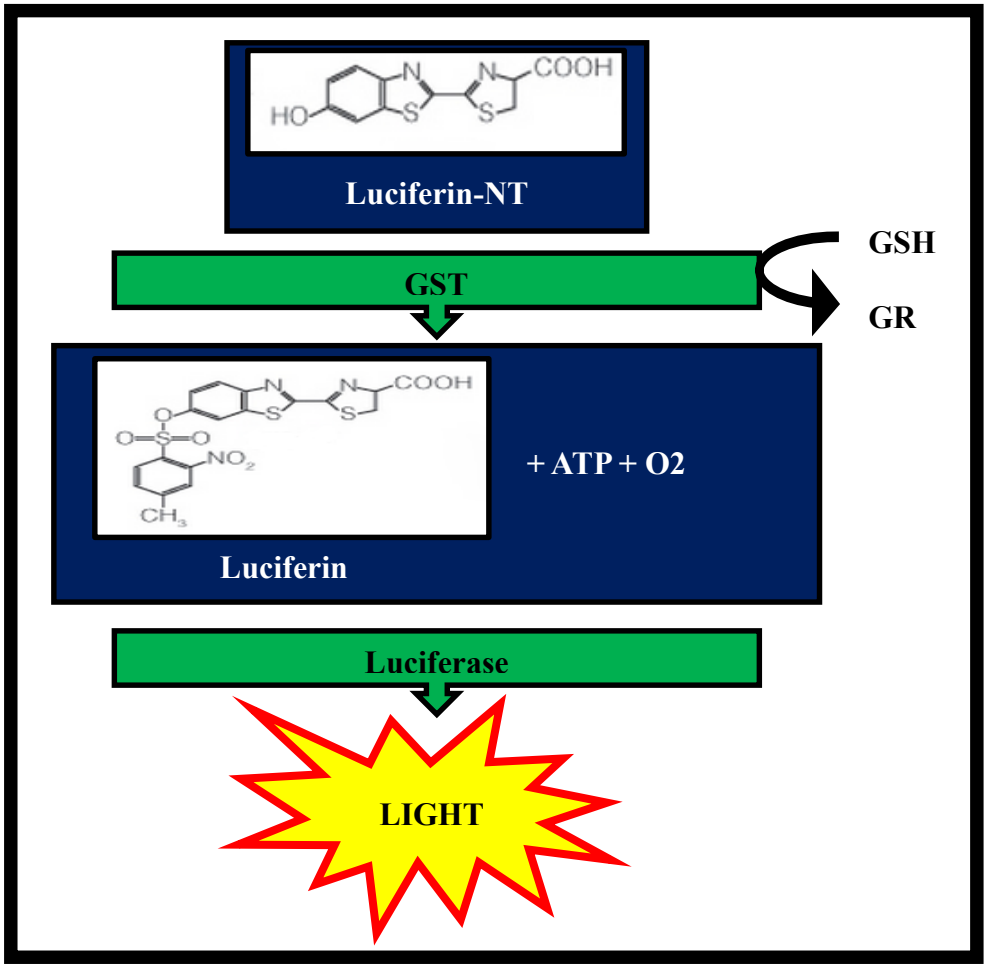

Figure 15: Principle of the GSH luminometry assay.

2.8 Comet assay

The comet assay is a sensitive method used to measure single and double DNA strand breaks. It was first described by Ostling and Johanson [81] and was subsequently modified by Singh et al [82]. These modifications involved the lysis of cells embedded in agarose using a lysis solution, containing a detergent and a high salt concentration, in an alkaline environment. The comet assay exploits the fact that DNA is supercoiled in nature and it is negatively charged. The phosphate ions present in the ribose-phosphate backbone of DNA confers a negative charge and allows for the migration of DNA towards the anode when subjected to electrophoresis in an alkaline solution. When strand breaks occur, DNA loses this supercoiled structure and the free ends are able to migrate towards the anode [83].

Low melting point agarose (LMPA) was used to prepare the gels. The first gel layer (700µl 1% LMPA) was formed on a frosted microscope slide, covered with a coverslip and incubated at 4°C (10min). Thereafter, the coverslip was removed, a second gel layer (1.5µl GR Red dye, 25µl cell suspension (10^4 cells) in 175µl 0.5% LMPA) was added, coverslips were placed over slides and incubated as above. Coverslips were removed and a third layer was added (0.5% LMPA, 200µl) onto the second. Once the third layer solidified, coverslips were removed, slides were submerged in an ice-cold cell lysing solution (10mM Tris (pH 10), 1% Triton X-100, 2.5M NaCl, 100mM EDTA and 10% DMSO) and incubated in the dark (4°C, 1hr).

After incubation, the lysing solution was removed, slides were placed in an electrophoresis tank filled with electrophoresis buffer (300mM NaOH and 1mM Na_2EDTA) and allowed to equilibrate for 20min. The electrophoresis tank was then sealed and a constant voltage was applied (25V, 35 minutes). After electrophoresis, slides were washed thrice (5min each) with neutralisation buffer (0.4M Tris, pH 7.4). The comet tails were visualised using an intercalating

dye, GR Red, an Olympus IX5I inverted fluorescent microscope (510-560nm excitation, 590nm emission filters) and analySIS Image Processing Software (Novell). Approximately 50 comets per treatment (3 replicates) were counted and analysed by measuring tail length (μm).

2.9 Quantitative polymerase chain reaction (qPCR)

PCR is sensitive, specific technique that can be used for the amplification and detection of nucleic acid sequences. This technique requires the following components:

- A DNA target sequence to be amplified
- Forward and reverse primers that are complementary to the 3' ends of the forward and reverse strands of the target sequence
- *Taq* DNA Polymerase, which catalyses the DNA synthesis process
- Deoxynucleoside triphosphates (dNTPs) that are used to synthesise new strands of DNA
- $MgCl_2$, which acts as a DNA stabiliser and is required for optimal functioning of Taq polymerase
- A specific buffer solution which maintains the required conditions, such as pH, during a PCR reaction

This technique requires the interaction of chemically synthesised primers that are complementary to the target DNA flanking sites, dNTPs and *Taq* DNA polymerase. The primers bind to the complementary flanking sites of the DNA template. DNA polymerase then incorporates dNTPs to the 3'-OH^- ends of the primers, thereby amplifying the target region.

There are three clear steps to a PCR reaction; 1) Denaturation, 2) Annealing and 3) Extension. To begin the PCR reaction, the temperature is raised to 95˚C so that denaturation can take place. This step ensures that the DNA double strand (dsDNA) is "melted" into DNA single

strands (ssDNA). The annealing step involves lowering the temperature to ±55˚C to allow the primers to bind to the target gene [84]. Primer binding provides DNA polymerase with a foundation to begin copying the DNA strand. The polymerase used is Taq polymerase, from the bacteria *Thermus aquaticus*. Taq polymerase is a thermostable enzyme that catalyses the synthesis of new DNA strands [85]. However, the optimum functioning temperature for Taq polymerase is 72˚C, thus the temperature is raised to 72˚C in the extension step to facilitate DNA synthesis [84]. These three steps conclude one cycle of a PCR reaction (Figure 16). This cycle is repeated 30 to 40 times to achieve acceptable amplification of the target sequence.

Conventional PCR successfully amplifies target DNA regions, but it does not quantify the sample. On the other hand, qPCR allows for the amplification and simultaneous quantification of the target gene in a sample. Firstly, RNA must be isolated and used to synthesise single stranded complementary DNA (cDNA) by reverse transcription. This cDNA is then used for qPCR. The qPCR cycles are similar to conventional PCR cycles (Figure 16), however, qPCR incorporates SYBR Green, a DNA-binding dye, which allows quantification to occur. The dye binds to DNA as amplification occurs and emits fluorescence as the cycles progress. A house-keeping gene is detected with the target gene in qPCR. This provides a control by which to measure the quantity of the amplified target gene. Data is analysed by comparing the target gene with the house-keeping gene and using the Livak and Schmittgen method of quantitation [86].

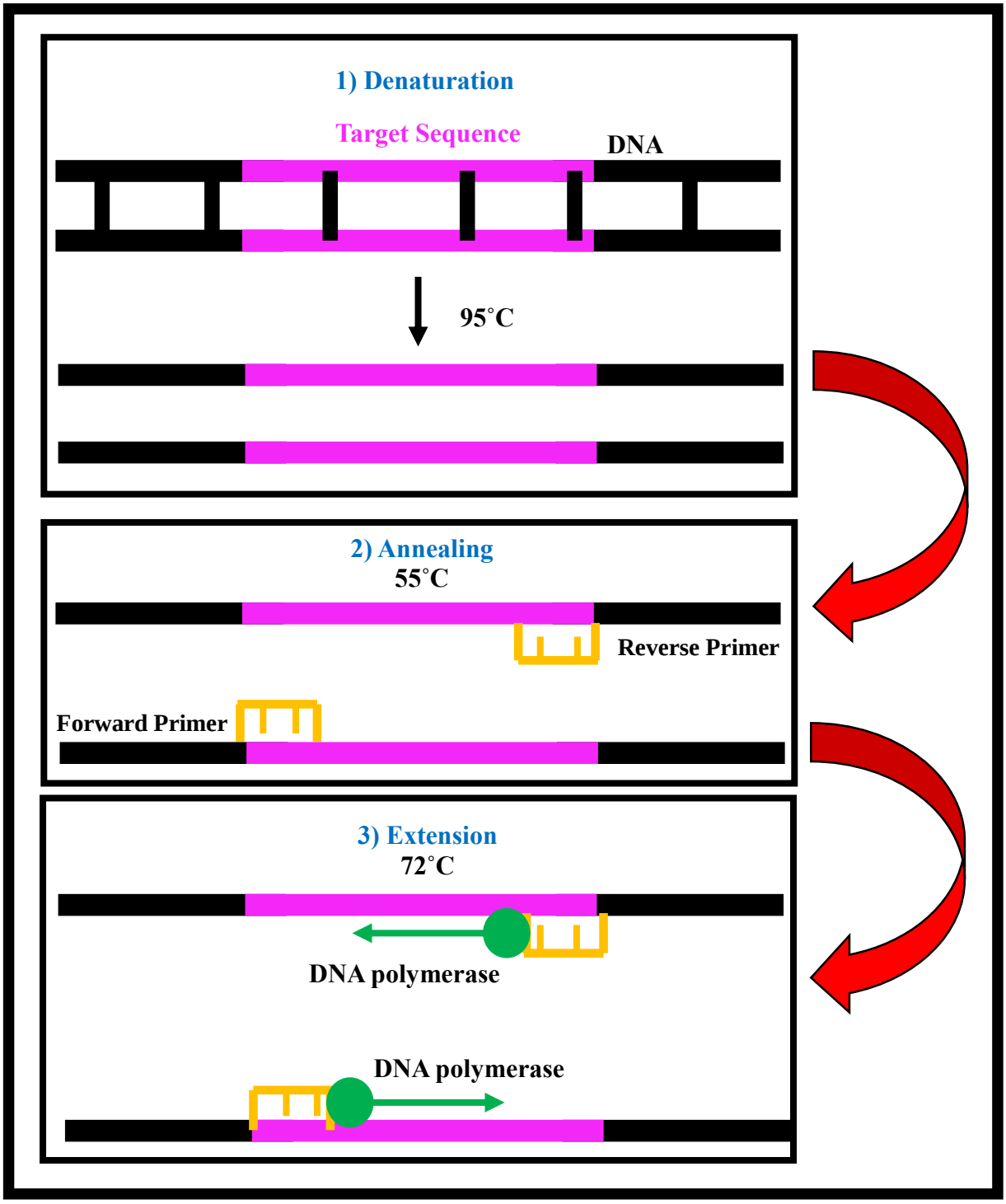

Figure 16: Representation of one cycle of the PCR target DNA amplification process.

2.9.1 RNA extraction

RNA was isolated following an in-house protocol using Trizol. Trizol reagent (500µl) was added to each flask and incubated (4ºC, 10min). Cells were removed from flasks, transferred

to eppendorfs and stored in Trizol at -80ºC overnight. Chloroform (100µl) was added to thawed samples and incubated (RT, 3min). Thereafter, cell suspensions were centrifuged (12,000*g*, 4ºC, 15min) and the aqueous phase was removed. Next 250µl isopropanol was added and samples were left overnight at -80ºC. Samples were thawed and centrifuged (12,000*g*, 4ºC, 20min). The supernatant was discarded, the pellet was retained and washed with 75% cold ethanol (500µl) and centrifuged (7,400*g*, 4ºC, 15min). Ethanol was removed and samples were allowed to air dry. The pellet was resuspended in nuclease-free water (15µl) and incubated (RT, 3min). The RNA was quantified using the Nanodrop2000 spectrophotometer and the A_{260}/A_{280} ratio was used to assess the RNA integrity. The concentration of RNA was standardised to 2500ng/µl and used to prepare cDNA.

2.9.2 cDNA Synthesis

The standardised RNA was used to synthesise cDNA using the iScript cDNA synthesis Kit (Bio-Rad) as per manufacturer's instructions. Briefly, tubes were prepared for each sample and a reaction mix was prepared. The reaction mix contained 4µl 5X iScript reaction mix, 1µl iScript reverse transcriptase, 11µl nuclease-free water and 4µl of each RNA sample was added to this solution. The tubes were then incubated in a thermocycler (GeneAmp® PCR System 9700, Applied Biosciences) for 40 minutes (5 minutes at 25˚C, 30 minutes at 42˚C and 5 minutes at 85˚C).

2.9.3 qPCR

Gene expression was analysed using the iScript SYBR Green PCR kit (Bio-Rad), according to the manufacturer's instructions. Each reaction volume totalled 25µl (12.5µl SYBR Green, 1µl forward primer, 1µl reverse primer, 9µl nuclease-free water and 1.5µl cDNA sample). The mRNA expressions of OGG1, CAT, SOD, GPX and Nrf2 was investigated using specific

primers (Table 1). This assay was carried out using 6 replicates per treatment and β-Actin as a house-keeping gene. The initial denaturation occurred at 95ºC (4min), followed by 37 denaturation cycles (95ºC, 15sec). An annealing step was then carried out for 40sec dependent on specific annealing temperatures of each gene (OGG1 - 60ºC; Nrf2, Cat and GPx - 58ºC; SOD - 57ºC). An extension step occurred (72ºC, 30 sec), followed by a plate read of 37 cycles (CFX96 Touch™ Real-Time PCR Detection System). The method described by Livak and Schmittgen was employed to determine the changes in relative mRNA expression, where $2^{-\Delta\Delta Ct}$ represents the fold change observed in mRNA expression [86].

Table 1: List of primer sequences used for qPCR

Primer	Primer Sequence
OGG1 sense	5'-GCATCGTACTCTAGCCTCCAC-3'
OGG1 antisense	5'-AGGACTTTGCTCCCTCCAC-3'
CAT sense	5'-TAAGACTGACCAGGGCATC-3'
CAT antisense	5'-CAACCTTGGTGAGATCGAA-3'
SOD sense	5'-GAGATGTTACACGCCCAGATAGC-3'
SOD antisense	5-AATCCCCAGCAGTGGAATAAGG-3'
GPx sense	5'-GACTACACCCAGATGAACGAGC-3'
GPx antisense	5'-CCCACCAGGAACTTCTCAAAG-3'
Nrf2 sense	5'-AGTGGATCTGCCAACTACTC-3'
Nrf2 antisense	5'-CATCTACAAACGGGAATGTCTG-3'
β-actin sense	5'-TGACGGGTCACCCACACTGTGCCCAT-3'
β-actin antisense	5'-CTAGAAGCATTTGCGGTGGACGATGGAGGG-3'

2.10 SDS-PAGE and Western Blotting

2.10.1 Protein isolation and sample preparation

Crude protein was isolated from cells using Cytobuster™ supplemented with phosphatase and protease inhibitors. Cytobuster reagent (250µl) was added to flasks following treatments; the cells were scraped, transferred to eppendorfs and incubated on ice for 10min. The cell solution was then centrifuged (10,000*g*, 4°C, 5min). The supernatant was used for protein quantification using the Bicinchoninic Acid (BCA) Assay. The BCA assay is a colorimetric assay used to determine the concentration of protein in each sample tested [87]. This assay functions by observing the formation of chromophores formed by a reaction between the BCA solution and cuprous ions (Cu^{1+}). Cuprous ions are produced during the interaction of proteins with alkaline Cu^{2+}, this is known as the biuret reaction (Figure 14) [87]. This assay can be used to determine protein concentration based on the intensity of the purple chromophore [88].

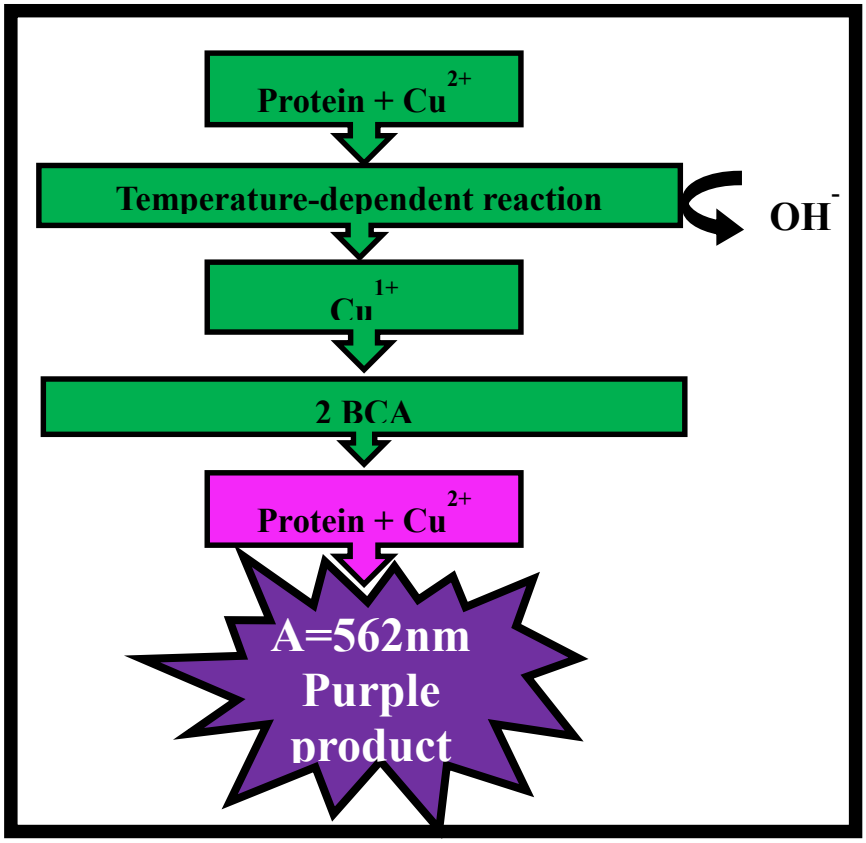

Figure 17: The reaction observed in the BCA assay during protein quantification.

Bovine Serum Albumin (BSA) standards (0-1mg/ml) were prepared. Samples and standards (25µl) were pipetted into a 96-well microtitre plate in duplicate. The BCA reagent was prepared in a ratio of 198µl BCA: 4µl $CuSO_4$ per reaction, and 200µl of this working solution was added to each well. The plate was incubated at 37°C for 30min, thereafter, the absorbance was read on a Bio-Tek MQx200 spectrophotometer (SA) at 562nm (Figure 15). A standard curve was constructed and proteins were standardised to 1mg/ml.

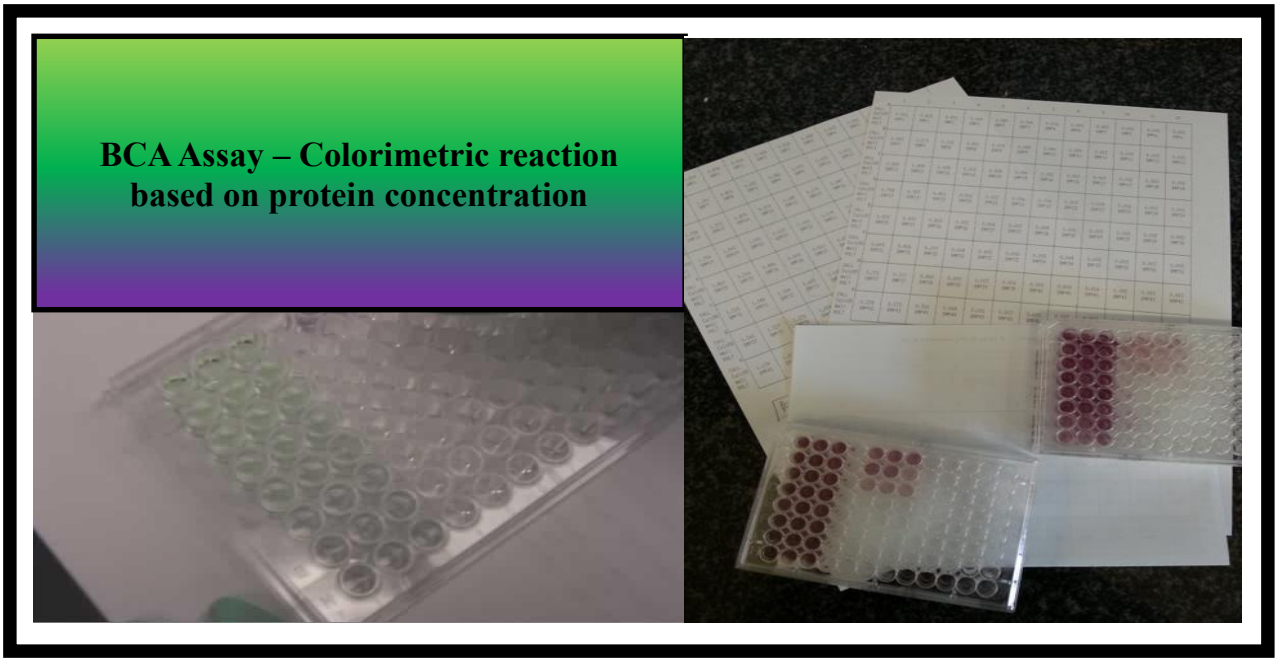

Figure 18: Colour changes seen in the BCA assay.

Laemmli buffer (dH2O, 0.5M Tris-HCl (pH 6.8), glycerol, 10% SDS, β-mercaptoethanol, 1% bromophenol blue) was added to each sample (1:1, total volume 200µl), and heated to 100°C (5min). This buffer is also known as the tris-glycine buffer system. The components each have specific functions; glycerol provides weight to the protein sample and allows the sample to settle at the bottom of the wells to prevent dissolution of the protein, β-mercaptoethanol cleaves disulfide bonds between molecules to allow for an elongated monomeric molecule and bromophenol blue acts as a tracking dye so visualisation of the dye front is possible.

2.10.2 SDS-Polyacrylamide gel electrophoresis (SDS-PAGE) and Transfer

The sodium dodecyl sulphate – polyacrylamide gel electrophoresis (SDS-PAGE) method was developed by Laemmli, he showed that proteins can be separated and observed during migration through a gel [89]. This method is extremely important and widely used in the biochemistry field. Proteins are separated according to their molecular weights by migrating through polyacrylamide gels [90]. These proteins are then transferred to nitrocellulose membranes and probed using antibodies [91]. The powerful detergent, SDS, serves two functions based on two functional areas, namely the hydrophobic (dodecyl) component and the highly charged (sulphate) component. The dodecyl section interacts with hydrophobic amino acids in proteins. The detergent elongates globular proteins into elongated molecules and confers negative charges along the length of the protein, thus facilitating migration towards a positive electrode. The percentage of polyacrylamide gel dictates the migration of proteins, since larger molecules do not migrate easily through high percentage acrylamide gels. This process removes the charge and shape of the protein as a variable, thus the migration depends entirely on molecular weight.

Protein samples were separated on SDS polyacrylamide gel (7.5% resolving gel and 4% stacking gel) for 1hr at 150V. Thereafter, the proteins were transferred onto nitrocellulose membranes using the Transblot® Turbo™ Transfer system (Bio-Rad). Nitrocellulose membranes and polyacrylamide gels are sandwiched between fibre pads, a current is passed through this and facilitates the transfer of proteins from the gels to membranes (Figure 16).

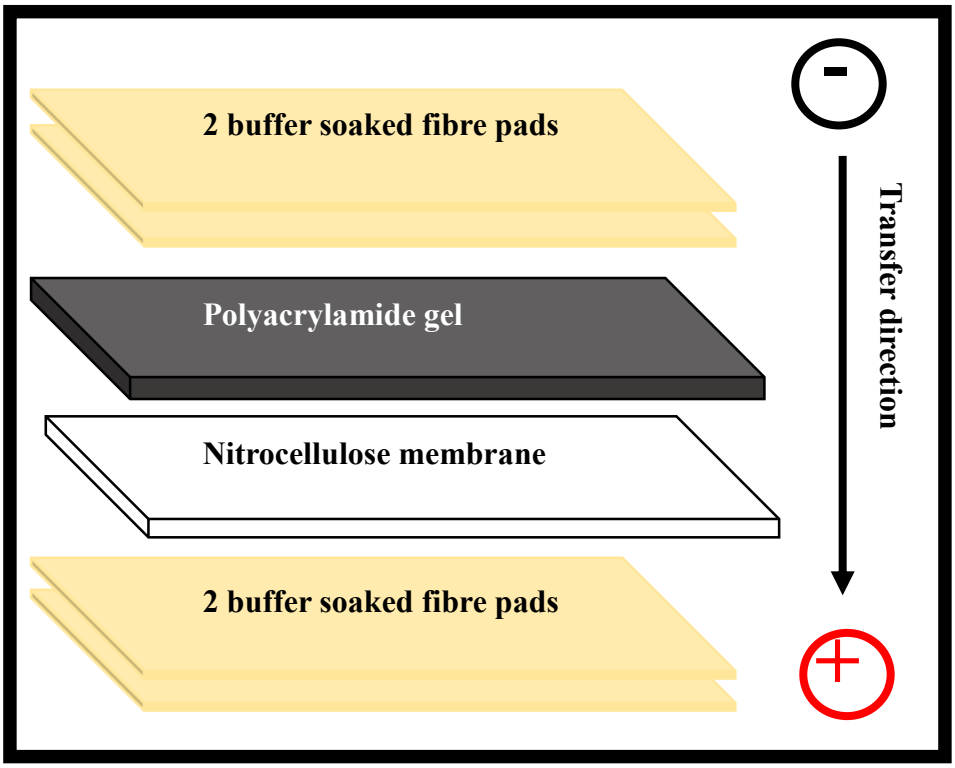

Figure 19: Components of the transfer system.

2.10.3 Western blotting

Proteins of interest can be detected by probing the nitrocellulose membranes with specific antibodies. Firstly, the membrane must be blocked with a BSA solution to prevent non-specific binding of the antibodies. Secondly, the membrane is incubated with a primary antibody against the specific protein of interest, this is followed by an incubation with a secondary HRP-conjugated antibody. The secondary antibody allows for the visualisation of the protein of interest during chemiluminescent analysis of the membrane (Figure 17).

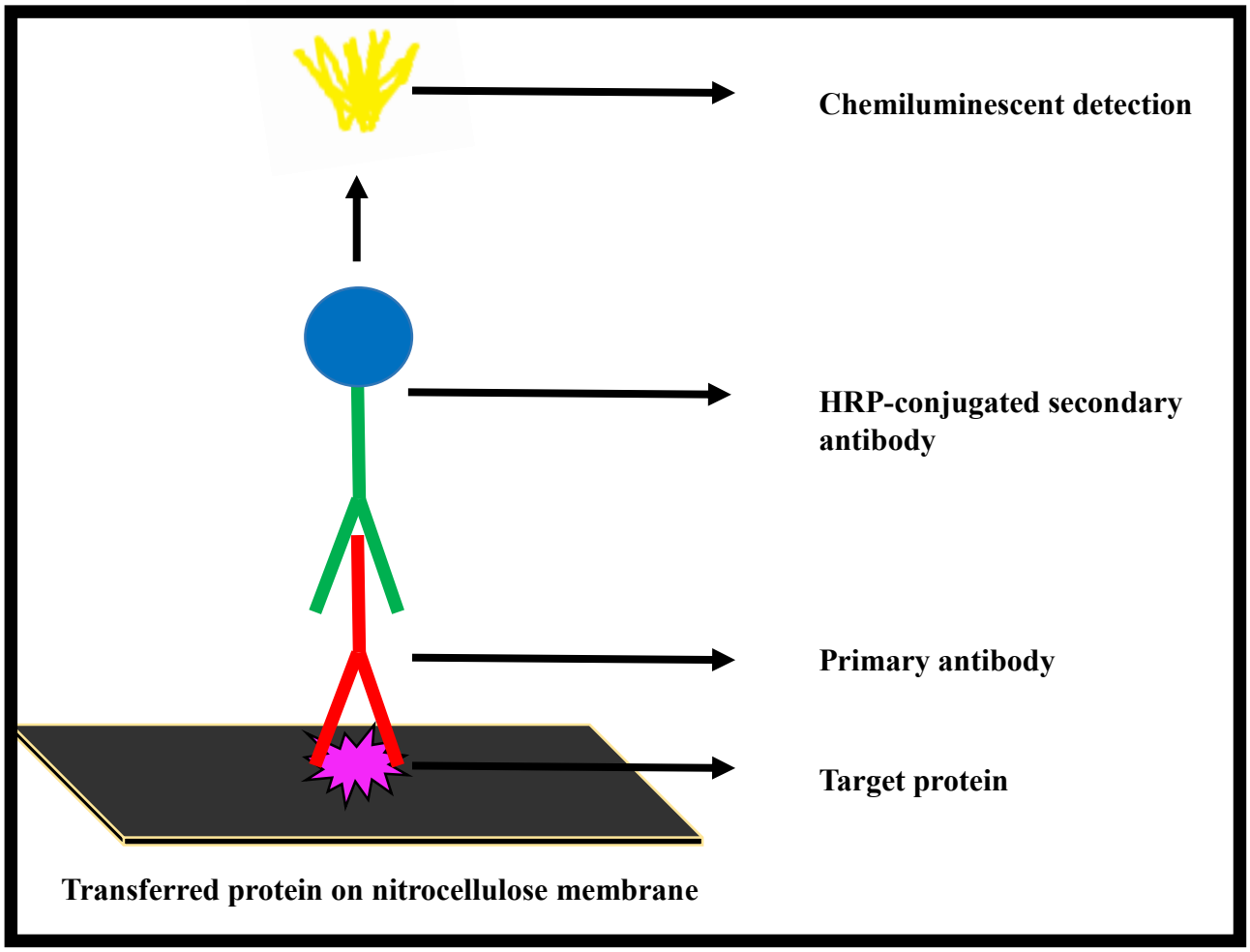

Figure 20: Chemiluminescent detection of the antibody-antigen reaction.

Membranes were blocked with 3% BSA in Tris buffered saline (TTBS, 25 mM Tris (pH 7.6) 150 mM NaCl, 0.05% Tween 20) for 30min, and incubated with a primary antibody (1:1,000, 3% BSA in TTBS at 4°C overnight). Antibodies used were anti-Nrf2 and anti-phospo SIRT1. Protein concentrations were standardised to anti-β-actin. After incubation, the primary antibody was removed, membranes were washed thrice with TTBS (10min) and incubated with a HRP-conjugated secondary antibody in 3% BSA (1:10,000) for 1hr. Following incubation, membranes were washed with TTBS. Clarity Western ECL Substrate (Bio-Rad) (400µl) was added to the membranes and images were captured using a gel documentation system (UviTech Alliance 2.7). The membranes were then quenched with hydrogen peroxide, incubated in a

blocking solution (3% BSA, 1hr, RT), rinsed twice in TTBS and probed with HRP-conjugated anti-β-actin (house-keeping protein). Densitometry analysis was performed using the UviTech Analysis software and protein expression was read as relative band intensity (RBI). Protein expression was reported as RBI of the protein of interest divided by the RBI of the loading control. The fold change was calculated by normalizing the RBI of the samples against the RBI of β-actin, this ratio was used to calculate the fold change.

2.11 Flow cytometry - Intracellular ROS

Fluorescence activated sell sorting (FACS) is carried out using a flow cytometer. This instrument is able to measure characteristics of individual cells flowing in a stream of fluid, using fluorescent probes and optical detectors [4]. Flow cytometry is able to detect intracellular ROS by measuring the fluorescence emitted per cell analysed. This emitted fluorescence is collected by optical detectors and specific wavelengths are isolated. The light is then converted to electrical pulses that can be analysed by a computer (Figure 21).

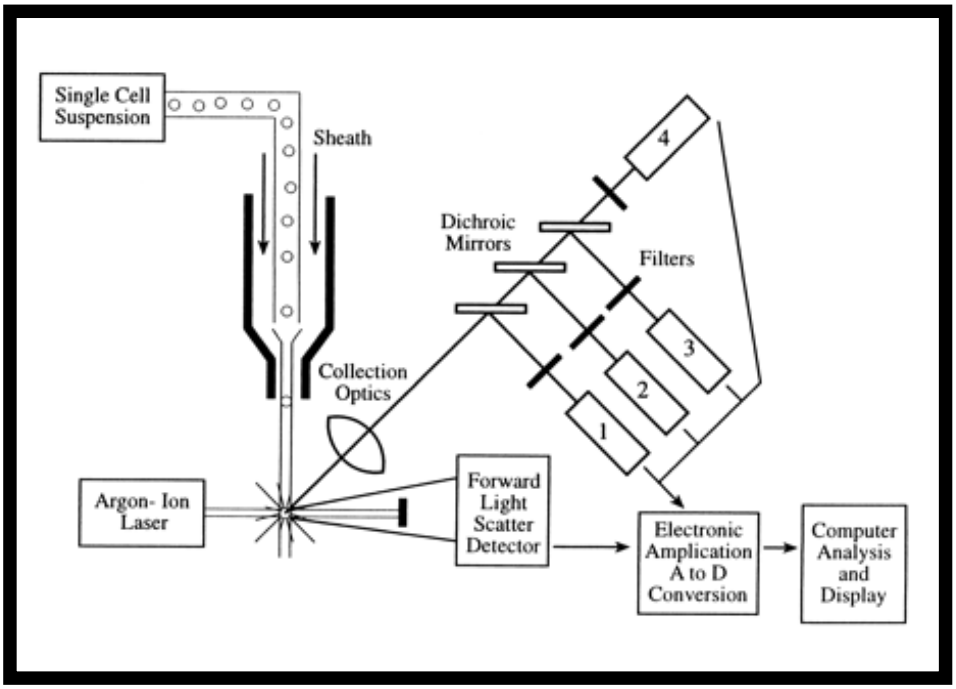

Figure 21: Flow cytometer components [4].

Dichlorodihydrofluorescein diacetate (DCFDA) (Santa Cruz Biotechnology) was used to detect intracellular ROS, since it is a cell permeant that reacts with superoxide, hydroxyl and peroxynitrite radicals. DCFDA passively diffuses into cells and is retained and cleaved by intracellular esterases. The DCFDA probe is non-fluorescent, however, upon oxidation by ROS, it is converted to a very fluorescent compound, 2', 7',-dichlorofluorescein (DCF). Intracellular ROS was determined following 24hr incubation with OTA and resveratrol. Treated cells were removed and counted as per assay requirement, (500,000 cells were required per treatment). Cells were incubated in phenol red free media, supplemented with 10% FCS and 10µM DCFDA, in the dark (45min, 37ºC). Thereafter, cells were rinsed thrice with 1.0M PBS and centrifuged (400*g*, RT, 5min). Once the washes were complete, the cells were suspended in 150µl 0.1M PBS and analysed using an Accuri™ C6 flow cytometer (Becton Dickinson). Live cells were gated and the fluorescence of DCF was measured (emission: 492-495nm; excitation: 517-527nm). A total of 50,000 events were acquired and analysed using CFlow Plus Software.

2.12 Statistical analysis

Statistical analyses were performed using a one-way analysis of variance (ANOVA) test and the Students' T-test, using GraphPad Prism version 5.0 (GraphPad Software, San Diego, California). All data is expressed as mean ± standard error of mean. All assays were run in triplicate and differences were considered statistically significant at values of $*p<0.05$.

Chapter 3

3. Results

3.1 MTT Assay

The MTT assay was used to determine an IC_{50} value of OTA in HEK293 cells after 24hr treatment (Figure 22). The resulting dose-response curve was used to calculate the IC_{50} of OTA which was used for all subsequent assays. Using this curve, the IC_{50} value was calculated as 1.5µM OTA.

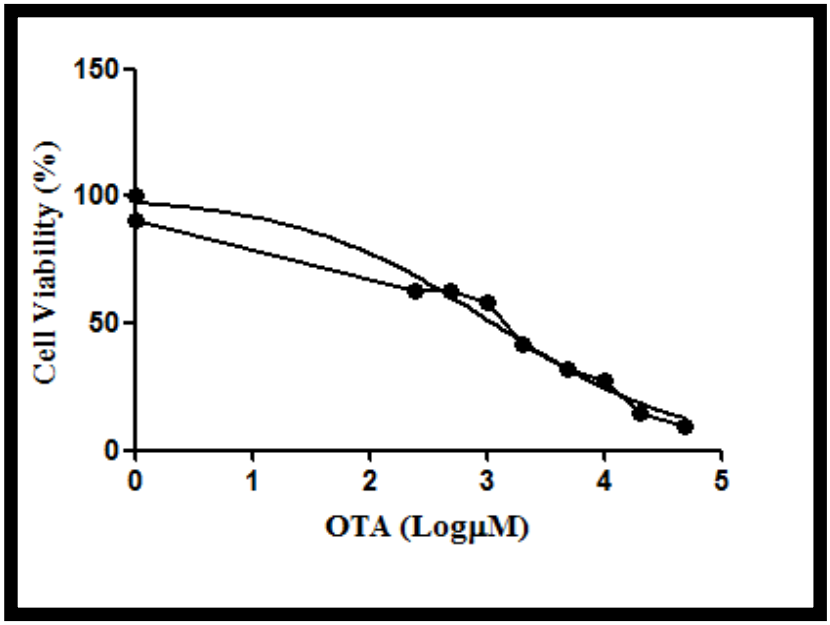

Figure 22: Percentage viability of cells exposed to OTA over 24 hours. An IC_{50} of 1.5µM was calculated from the dose-response curve.

3.2 Analysis of Intracellular ROS

Flow cytometry was used to measure intracellular ROS production (Figure 2). These results showed that resveratrol significantly reduced intracellular ROS in HEK293 cells (p<0.0001). Both the OTA and OTA+Resveratrol treatments significantly reduced ROS when compared to

control cells ((Figure 2); p=0.0048). This result indicates that resveratrol aids in significantly reducing the oxidative stress placed on the cell.

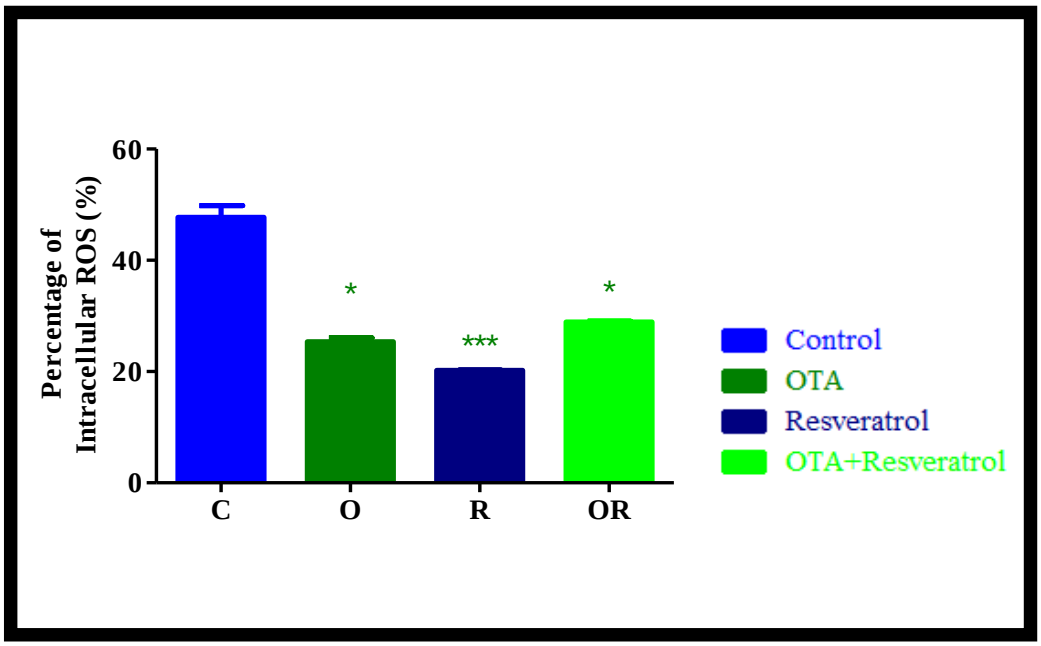

Figure 23: Resveratrol (25µM) significantly decreased the percentage of intracellular ROS (***p<0.0001), while OTA and OTA+Resveratrol treatments decreased the values of ROS when compared to control cells (*p=0.0048).

3.3 Assessment of DNA damage and repair

Resveratrol has been shown to significantly reduce the extent of DNA damage resulting from exposure to OTA. Comet tails were significantly longer in OTA-treated cells (44.81 ± 1.516; p<0.0001), as compared to the controls (Figure 3). In contrast, resveratrol significantly decreased comet tail lengths compared to all other treatments ((Figure 3); 11.69 ± 0.695; p<0.0001). Interestingly, cells co-treated with OTA+Resveratrol showed significantly decreased comet tail lengths as compared to cells only exposed to OTA ((Figure 3); 29.03 ± 1.110 vs 44.81 ± 1.516; p<0.0001). OTA significantly increased the mRNA expression of OGG1, a DNA glycosylase enzyme, while resveratrol significantly decreased its expression ((Figure 3); p=0.0294). However, OTA+Resveratrol co-treated cells significantly increased

OGG1 expression, strongly suggesting a synergistic effect on the expression of this DNA repair enzyme ((Figure 3); p=0.0027) A plausible explanation for this may be that increased comet tail lengths (Figure 3A) may trigger a protective mechanism by upregulation of OGG1.

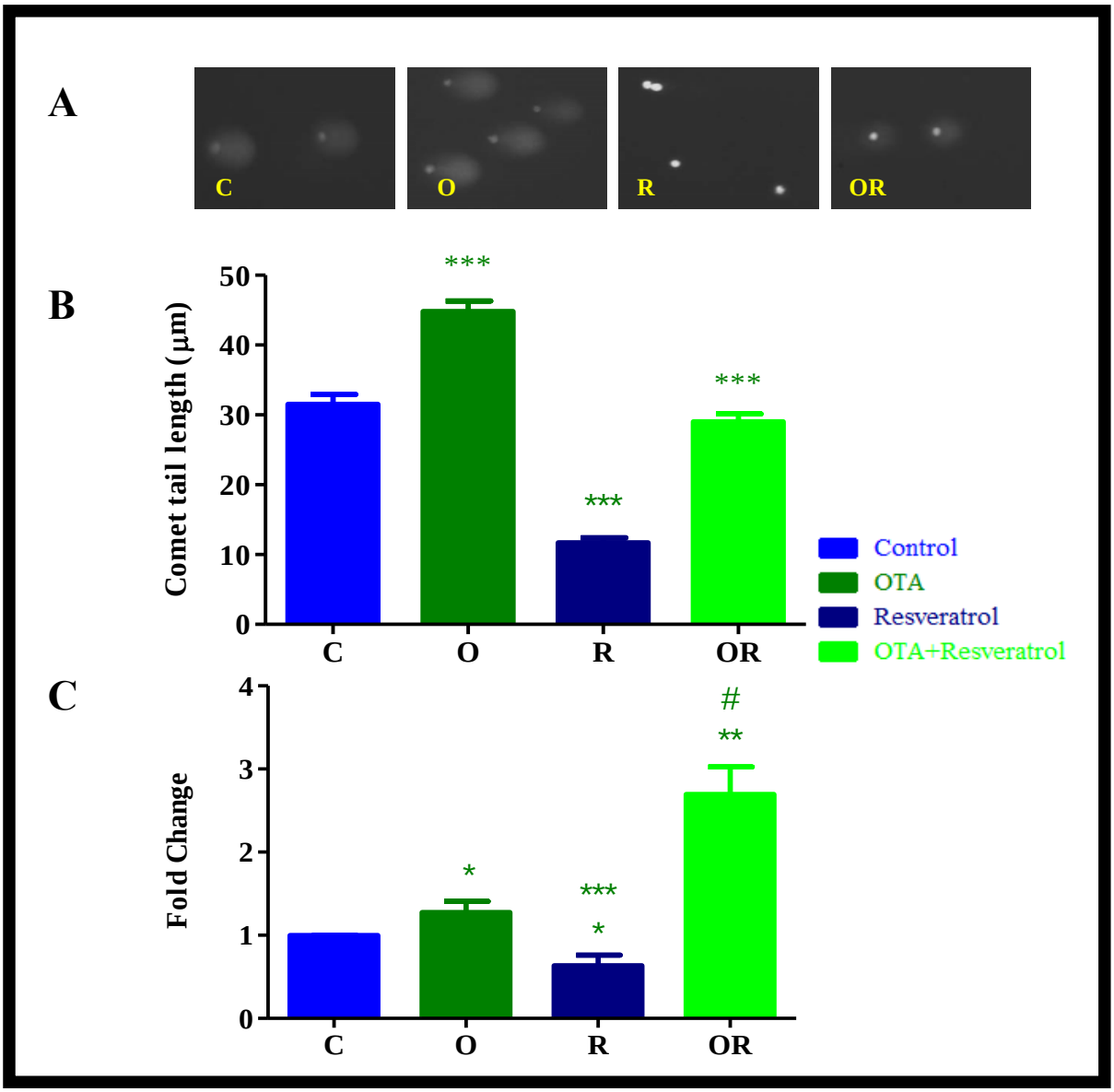

Figure 24: Assessment of DNA damage showing images of A) comet tails and B) the measurement of comet tail lengths. OTA increased comet tail lengths (***p<0.0001), while resveratrol significantly decreased lengths (***p<0.0001). C) The fold change analysis of OGG1 mRNA expression in cells exposed to OTA and resveratrol indicates that OTA significantly increased, while resveratrol significantly decreased expression of OGG1 mRNA

(p<0.05). OTA+Resveratrol co-treated cells showed a significant increase in OGG1 mRNA expression when compared to OTA-exposed cells, which correlates to the events seen in the comet assay.

3.4 Measurement of GSH and GSSG concentrations

Intracellular concentration of GSH and GSSG was determined using luminometry. Cells co-treated with OTA+Resveratrol significantly increased concentrations of both GSH and GSSG compared to other treatments (p=0.0117). In contrast, resveratrol-treated cells contained low concentrations of GSH, and high concentrations of GSSG when compared to control and OTA-treated cells (Figure 25).

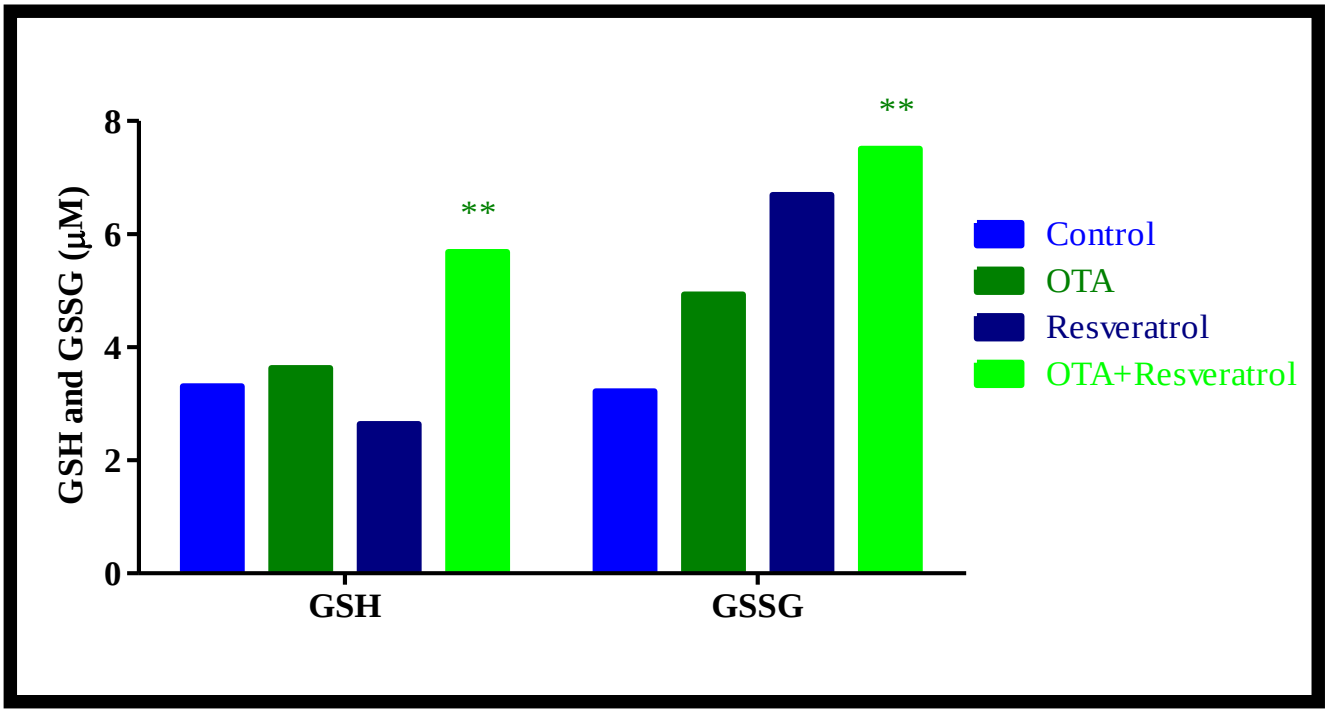

Figure 25: Concentrations of GSH and GSSG in HEK293 cells after exposure to OTA and resveratrol. The OTA+Resveratrol co-treatment increased the concentrations of GSH and GSSG (**p=0.0117), while resveratrol decreased GSH concentrations.

3.5 qPCR analysis of antioxidant response

The mRNA expression of genes associated with the antioxidant response was assessed by qPCR. The expression of Nrf2, an antioxidant defence regulator, was significantly increased by both OTA and resveratrol ((Figure 5A); p=0.0048) and OTA+Resveratrol (p<0.0001). The antioxidant enzyme gene expressions of GPx ((Figure 5B); p=0.0048), CAT ((Figure 5C); p=0.0048) and SOD ((Figure 5D); p=0.0048) were significantly increased by both OTA and resveratrol.

Also, the co-treatment of OTA+Resveratrol induced a greater increase in GPx (p=0.0002), CAT (p=0.0003) and SOD (p=0.0003) than observed in other treatments. These results show that resveratrol has greatly increased the antioxidant defence of the cell.

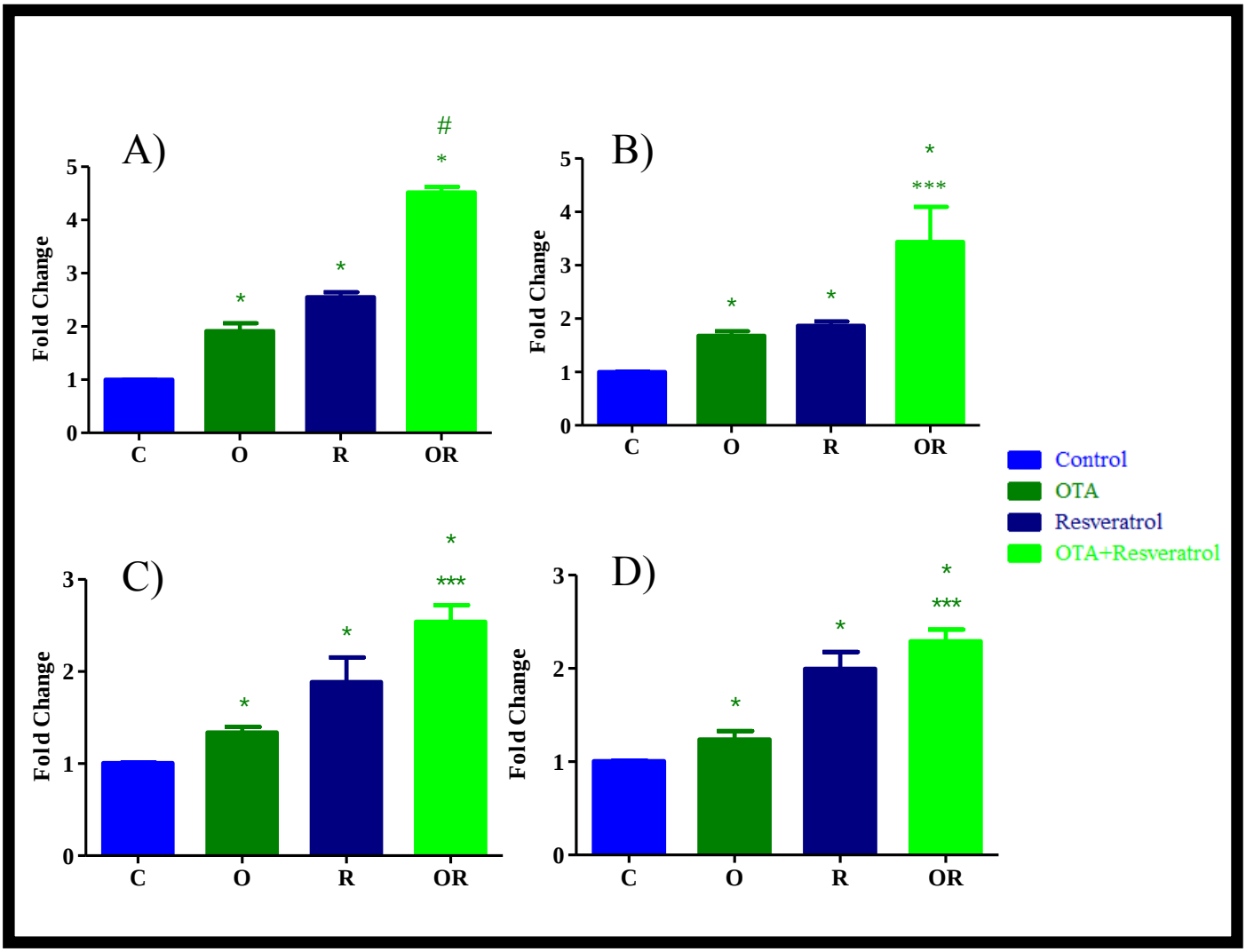

Figure 26: OTA, resveratrol and OTA+Resveratrol significantly increased the mRNA expression of genes associated with the antioxidant response in HEK293 cells – A) Nrf2 (*p<0.05), B) GPx (*p<0.05), C) CAT (*p<0.05) and D) SOD (*p<0.05).

3.6 Western blotting

The protein levels of Nrf2 and pSIRT1 was determined using western blotting. Nrf2 protein expression was significantly decreased by resveratrol and OTA+Resveratrol ((Figure 6); p=0.0048 and p=0.0002 respectively). Phosphorylation of SIRT1 protein in both resveratrol and OTA+Resveratrol treatments was significantly increased ((Figure 6); p=0.0048 and

p=0.0002 respectively), indicating that resveratrol had exerted its influence on the activation of SIRT1 proteins.

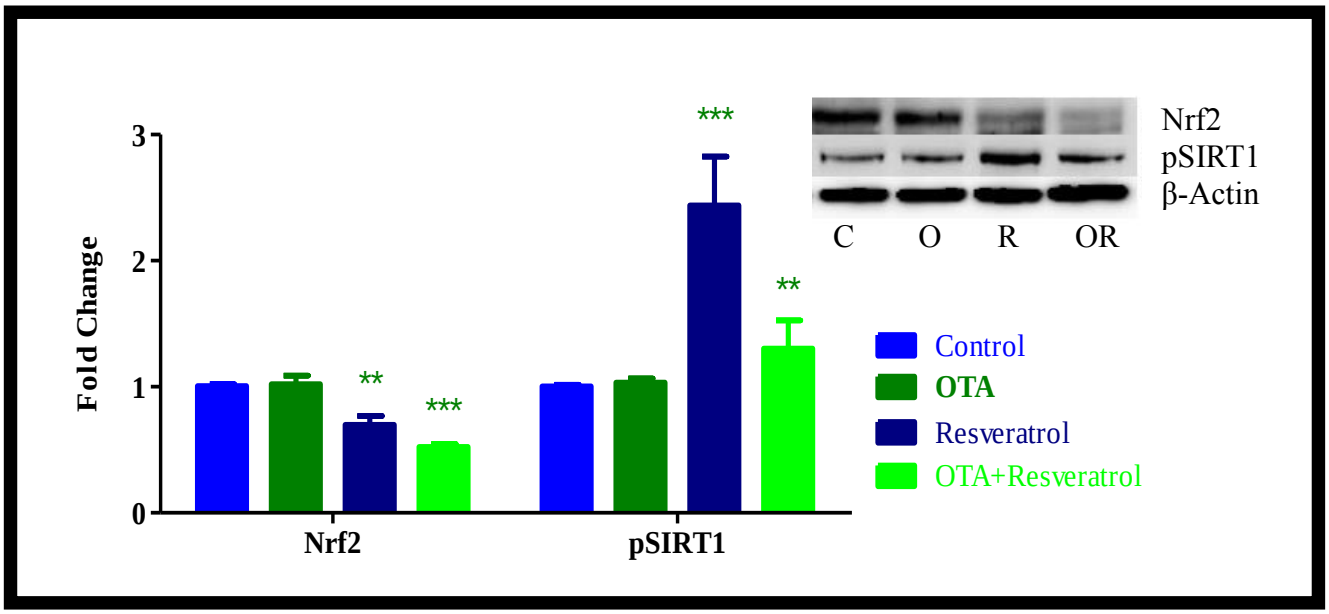

Figure 27: Western blot images and relative fold change in protein levels of Nrf2 and pSIRT1 in response to OTA and resveratrol exposure. Resveratrol and OTA+Resveratrol significantly decreased the expression of Nrf2 (***p*<0.05). Resveratrol and OTA+Resveratrol significantly increased the levels of pSIRT1 (****p*=0.0002 and ***p*<0.05 respectively), indicating increased activation of SIRT1.

Chapter 4

4. Discussion

OTA is a mycotoxin that frequently contaminates a wide range of foods. Once ingested OTA exerts its toxic effects via several pathways; one such pathway in the kidney is the increase in oxidative stress, resulting in DNA damage and progressive renal failure in individuals who chronically ingest foods contaminated with high concentrations of OTA [1]. OTA poses a health risk to populations in developing countries, as they depend largely on agricultural crops often heavily contaminated with fungi, such as *Aspergillus* and *Penicillium* [27]. OTA has been identified as an aetiological agent in BEN [27]. The exact mechanism of OTA toxicity is still relatively unknown and in this study we provide insight into the biochemical changes induced by OTA in HEK293 kidney cells.

Resveratrol is a phytoalexin commonly produced in grape skins as a result of damage or infection with *Botrytis cinerea*, a fungus known to contaminate grape crops [16]. This compound is known to have antioxidant characteristics and chemo-preventive potential, and has been proposed as a treatment for illnesses, such as cardiovascular disease, diabetes and cancer [92]. We determined whether resveratrol could prevent cytotoxicity induced by OTA in kidney cells.

Under normal conditions ROS serves to regulate intracellular signaling, however, under conditions of excessive ROS production, intracellular signaling is compromised and irreversible cellular damage can occur [29]. Oxidative stress will result in cytotoxicity and altered cellular functioning [73]. Lipids, proteins and DNA are susceptible to ROS attack and subsequent damage [30].

OTA decreased intracellular ROS (as determined by FACS), but induced single strand DNA breaks as seen in the comet assay. Acute exposure to OTA (1.5μM) resulted in significant DNA strand breaks in HEK293 cells, suggesting that OTA is genotoxic. In comparison to control cells, OTA significantly increased the lengths of comet tails, while resveratrol significantly decreased comet tail lengths by 63% and also limited damage by OTA, as observed in the OTA+Resveratrol effects. The co-treatment resulted in decreased comet tail lengths when compared to controls, and significantly decreased comet tail lengths by 35% compared to OTA-treated cells. Also, the percentage of intracellular ROS was lowest in resveratrol-treated cells. When cellular DNA damage occurs, the cell activates DNA repair enzymes, such as OGG1 – a DNA glycosylase. The mRNA expression of OGG1 was increased. OGG1 removes 8-oxoguanine base lesions, which could possibly result in mutations and carcinogenesis if left to accumulate [11]. The HEK293 cells increased the expression of OGG1 in response to OTA-induced DNA damage, as observed by the increased comet tail lengths. However, OGG1 expression was lowest in resveratrol-treated cells with shortest comet tails, while the OTA+Resveratrol co-treatment induced the highest expression of OGG1, coupled with a significant decrease in comet tail length. The co-treatment of OTA+Resveratrol seemed to synergistically increase the expression of OGG1 that may have afforded a protective function, and this is evidenced by shorter comet tails. The protective role of resveratrol over DNA (single/double strand breaks) can be attributed to its decrease in both intracellular ROS and OGG1 expression, thus providing evidence for its protective role and its possible anti-cancer potential.

GSH is an important co-factor required for GPx functionality, as it prevents excessive oxidative stress accumulation [76]. The OTA+Resveratrol co-treatment significantly increased concentrations of intracellular GSH and GSSG, suggesting that resveratrol is active in the

regeneration of GSH. This observation is further substantiated in cells that received resveratrol-only had higher concentrations of total GSH than the control and OTA-treated cells.

In addition, resveratrol significantly increased Nrf2 mRNA expression in all treatments, suggesting that resveratrol upregulates the antioxidant defence. Nrf2 activates the ARE and influences the increased transcription of detoxification enzymes, such as CAT, SOD and GPx. Resveratrol significantly increased mRNA expression of SOD, CAT and GPx in all treatments. GPx upregulation will increase GSH concentrations, whilst superoxide radicals, such as H_2O_2 is detoxified by SOD; CAT and GPx together then convert H_2O_2 into water [73]. This two-part reaction allows for the conversion of toxic species into natural by-products that can be used by the cell or easily removed [73].

Nrf2 protein expression however, did not correspond to Nrf2 mRNA expressions. This disparity may be attributed to the known protein synthesis inhibitory properties of OTA [93]. Although resveratrol attempts to repair the oxidative damage by increasing production of Nrf2 protein, OTA suppresses this attempt. The decreased Nrf2 expression strongly suggests that resveratrol itself mediates the antioxidant defence response, in keeping with its antioxidant properties [64]. Resveratrol is known to activate SIRT1, an NAD^+-dependent deacetylase. SIRT1 has been identified as a positive contributor in many regulatory pathways, such as cellular stress response and apoptosis [53]. Protein expression of pSIRT1 was significantly increased in both resveratrol treatments. Phosphorylation of SIRT1 results in increased nuclear localization of the protein, as well as increased enzymatic activity [94]. The stress protection pathway is mediated by SIRT1, increased phosphorylation would influence this function and induce deacetylation of stress proteins, such as p53 and PGC-1alpha, causing cellular protection and survival [95].

Chapter 5

5. Conclusion

This data provides insight into the workings of the toxin; we are proposing that short term effects of OTA contribute to its toxicity. The cells experience a significant increase in the antioxidant response due to the recognition of a cytotoxic environment, however, it is not possible to sustain an increased protective response while DNA damage occurs. Our data suggests that OTA exhausts the cell's antioxidant reservoir during acute exposure and thus the cell is left vulnerable as the exposure period continues.

Taken together, this data suggests resveratrol could be used as a potential treatment for OTA toxicity, as well as a possible therapy for other oxidative stress inducing toxins. Regarding the information on DNA damage prevention, this research also attests to the potential chemo-preventive attributes of resveratrol. Based on these findings, it would be worthwhile to further investigate the effects of OTA and explore the DNA repair properties of resveratrol in an *in vivo* model.

References

1. Pfohl-Leszkowicz A, Manderville RA: Ochratoxin A: An overview on toxicity and carcinogenicity in animals and humans. *Molecular Nutrition & Food Research* 2007, 51(1):61-99.
2. Halliwell B, Chirico S: Lipid peroxidation: its mechanism, measurement, and significance. *The American journal of clinical nutrition* 1993, 57(5 Suppl):715S-724S; discussion 724S-725S.
3. Baur JA: Resveratrol, sirtuins, and the promise of a DR mimetic. *Mechanisms of ageing and development* 2010, 131(4):261-269.
4. Brown M, Wittwer C: Flow Cytometry: Principles and Clinical Applications in Hematology. *Clinical Chemistry* 2000, 46(8):1221-1229.
5. Marin-Kuan M, Cavin C, Delatour T, Schilter B: Ochratoxin A carcinogenicity involves a complex network of epigenetic mechanisms. *Toxicon* 2008, 52(2):195-202.
6. Schilter B, Marin-Kuan M, Delatour T, Nestler S, Mantle P, Cavin C: Ochratoxin A: Potential epigenetic mechanisms of toxicity and carcinogenicity. *Food Additives & Contaminants* 2005, 22(sup1):88-93.
7. Bankole S, Schollenberger M, Drochner W: Mycotoxins in food systems in Sub Saharan Africa: A review. *Mycotoxin Research* 2006, 22(3):163-169.
8. van der Merwe KJ, Steyn PS, Fourie L, Scott DB, Theron JJ: Ochratoxin A, a toxic metabolite produced by Aspergillus ochraceus Wilh. *Nature* 1965, 205(976):1112-1113.
9. Jonsyn-Ellis F: Ochratoxin a: Any Cause for Concern in Sub Saharan Africa? *Science Journal of Environmental Engineering Research* 2012, Volume 2012:5.

10. Hohler D, Sudekum KH, Wolffram S, Frohlich AA, Marquardt RR: Metabolism and excretion of ochratoxin A fed to sheep. *Journal of animal science* 1999, 77(5):1217-1223.

11. Cheng Y, Ren X, Gowda AS, Shan Y, Zhang L, Yuan Y-S, Patel R, Wu H, Huber-Keener K, Yang JW: Interaction of Sirt3 with OGG1 contributes to repair of mitochondrial DNA and protects from apoptotic cell death under oxidative stress. *Cell Death and Disease* 2013, 4.

12. Özçelik N, Soyöz M, Kılınç İ: Effects of ochratoxin a on oxidative damage in rat kidney: protective role of melatonin. *Journal of Applied Toxicology* 2004, 24(3):211-215.

13. Schaaf GJ, Nijmeijer SM, Maas RF, Roestenberg P, de Groene EM, Fink-Gremmels J: The role of oxidative stress in the ochratoxin A-mediated toxicity in proximal tubular cells. *Biochimica et biophysica acta* 2002, 1588(2):149-158.

14. Meyer JN, Leung MCK, Rooney JP, Sendoel A, Hengartner MO, Kisby GE, Bess AS: Mitochondria as a Target of Environmental Toxicants. *Toxicological Sciences* 2013.

15. Nguyen T, Nioi P, Pickett CB: The Nrf2-antioxidant response element signaling pathway and its activation by oxidative stress. *The Journal of biological chemistry* 2009, 284(20):13291-13295.

16. Athar M, Back JH, Tang X, Kim KH, Kopelovich L, Bickers DR, Kim AL: Resveratrol: a review of preclinical studies for human cancer prevention. *Toxicology and applied pharmacology* 2007, 224(3):274-283.

17. Baur JA, Sinclair DA: Therapeutic potential of resveratrol: the in vivo evidence. *Nature reviews Drug discovery* 2006, 5(6):493-506.

18. Borra MT, Smith BC, Denu JM: Mechanism of Human SIRT1 Activation by Resveratrol. *Journal of Biological Chemistry* 2005, 280(17):17187-17195.

19. Timmers S, Auwerx J, Schrauwen P: The journey of resveratrol from yeast to human. *Aging* 2012, 4(3):146-158.

20. Creppy EE, Baudrimont I, Betbeder AM: Prevention of nephrotoxicity of ochratoxin A, a food contaminant. *Toxicology letters* 1995, 82-83:869-877.

21. Bayman P, Baker JL, Doster MA, Michailides TJ, Mahoney NE: Ochratoxin production by the Aspergillus ochraceus group and Aspergillus alliaceus. *Applied and environmental microbiology* 2002, 68(5):2326-2329.

22. Cavin C, Delatour T, Marin-Kuan M, Holzhauser D, Higgins L, Bezencon C, Guignard G, Junod S, Richoz-Payot J, Gremaud E: Reduction in antioxidant defenses may contribute to ochratoxin A toxicity and carcinogenicity. *Toxicological sciences : an official journal of the Society of Toxicology* 2007, 96(1):30-39.

23. Grosse Y, Baudrimont I, Castegnaro M, Betbeder AM, Creppy EE, Dirheimer G, Pfohl-Leszkowicz A: Formation of ochratoxin A metabolites and DNA-adducts in monkey kidney cells. *Chemico-biological interactions* 1995, 95(1-2):175-187.

24. Walker R: Risk assessment of ochratoxin: current views of the European Scientific Committee on Food, the JECFA and the Codex Committee on Food Additives and Contaminants. *Advances in experimental medicine and biology* 2002, 504:249-255.

25. Ramyaa P, Padma VV: Ochratoxin-induced toxicity, oxidative stress and apoptosis ameliorated by quercetin--modulation by Nrf2. *Food and chemical toxicology : an international journal published for the British Industrial Biological Research Association* 2013, 62:205-216.

26. O'Brien E, Dietrich DR: Ochratoxin A: the continuing enigma. *Critical reviews in toxicology* 2005, 35(1):33-60.

27. Castegnaro M, Canadas D, Vrabcheva T, Petkova-Bocharova T, Chernozemsky IN, Pfohl-Leszkowicz A: Balkan endemic nephropathy: role of ochratoxins A through biomarkers. *Molecular Nutrition & Food Research* 2006, 50(6):519-529.

28. Encyclopædia Britannica Online sv: "Balkans". 2014.

29. Wang CH, Wu SB, Wu YT, Wei YH: Oxidative stress response elicited by mitochondrial dysfunction: implication in the pathophysiology of aging. *Experimental biology and medicine* 2013, 238(5):450-460.

30. Marin-Kuan M, Ehrlich V, Delatour T, Cavin C, Schilter B: Evidence for a Role of Oxidative Stress in the Carcinogenicity of Ochratoxin A. *Journal of Toxicology* 2011, 2011.

31. Chu FS, Wilson BJ: Studies on Ochratoxins. *Critical reviews in toxicology* 1973, 2(4):499-524.

32. Ringot D, Chango A, Schneider YJ, Larondelle Y: Toxicokinetics and toxicodynamics of ochratoxin A, an update. *Chemico-biological interactions* 2006, 159(1):18-46.

33. Cooke MS, Evans MD, Dizdaroglu M, Lunec J: Oxidative DNA damage: mechanisms, mutation, and disease. *FASEB journal : official publication of the Federation of American Societies for Experimental Biology* 2003, 17(10):1195-1214.

34. Sorrenti V, Di Giacomo C, Acquaviva R, Barbagallo I, Bognanno M, Galvano F: Toxicity of Ochratoxin A and Its Modulation by Antioxidants: A Review. *Toxins* 2013, 5(10):1742-1766.

35. Brini M, Cali T, Ottolini D, Carafoli E: Intracellular calcium homeostasis and signaling. *Metal ions in life sciences* 2013, 12:119-168.

36. Creppy EE, Chakor K, Fisher MJ, Dirheimer G: The myocotoxin ochratoxin A is a substrate for phenylalanine hydroxylase in isolated rat hepatocytes and in vivo. *Archives of toxicology* 1990, 64(4):279-284.

37. Zanic-Grubisic T, Zrinski R, Cepelak I, Petrik J, Radic B, Pepeljnjak S: Studies of ochratoxin A-induced inhibition of phenylalanine hydroxylase and its reversal by phenylalanine. *Toxicology and applied pharmacology* 2000, 167(2):132-139.

38. Kumagai S, Aibara K: Intestinal absorption and secretion of ochratoxin A in the rat. *Toxicology and applied pharmacology* 1982, 64(1):94-102.

39. Roth A, Chakor K, Creppy EE, Kane A, Roschenthaler R, Dirheimer G: Evidence for an enterohepatic circulation of ochratoxin A in mice. *Toxicology* 1988, 48(3):293-308.

40. Anders MW: Metabolism of drugs by the kidney. *Kidney international* 1980, 18(5):636-647.

41. Pitout MJ: The hydrolysis of ochratoxin a by some proteolytic enzymes. *Biochemical Pharmacology* 1969, 18(2):485-491.

42. Xiao H, Madhyastha S, Marquardt RR, Li S, Vodela JK, Frohlich AA, Kemppainen BW: Toxicity of ochratoxin A, its opened lactone form and several of its analogs: structure-activity relationships. *Toxicology and applied pharmacology* 1996, 137(2):182-192.

43. Heussner AH, O'Brien E, Dietrich DR: Effects of repeated ochratoxin exposure on renal cells in vitro. *Toxicology in vitro : an international journal published in association with BIBRA* 2007, 21(1):72-80.

44. Takaoka M: The Synthesis of Resveratrol and its Derivatives. *Proceedings of the Imperial Academy* 1940, 16(8):405-407.

45. Takaoka M: The Phenolic Substances of White Hellebore (Veratrum Grandiflorum Loes. Fill). V Synthesis of Resveratrol (3, 5, 4-Trioxystilbene) and its Derivatives. *NIPPON KAGAKU KAISHI* 1940, 61(10):1067-1069.

46. Langcake P, Cornford CA, Pryce RJ: Identification of pterostilbene as a phytoalexin from Vitis vinifera leaves. *Phytochemistry* 1979, 18(6):1025-1027.

47. Fremont L: Biological effects of resveratrol. *Life sciences* 2000, 66(8):663-673.

48. Walle T, Hsieh F, DeLegge MH, Oatis JE, Jr., Walle UK: High absorption but very low bioavailability of oral resveratrol in humans. *Drug metabolism and disposition: the biological fate of chemicals* 2004, 32(12):1377-1382.

49. Leonard SS, Xia C, Jiang BH, Stinefelt B, Klandorf H, Harris GK, Shi X: Resveratrol scavenges reactive oxygen species and effects radical-induced cellular responses. *Biochemical and biophysical research communications* 2003, 309(4):1017-1026.

50. Fauconneau B, Waffo-Teguo P, Huguet F, Barrier L, Decendit A, Merillon JM: Comparative study of radical scavenger and antioxidant properties of phenolic compounds from Vitis vinifera cell cultures using in vitro tests. *Life sciences* 1997, 61(21):2103-2110.

51. Catalgol B, Batirel S, Taga Y, Ozer NK: Resveratrol: French Paradox Revisited. *Frontiers in Pharmacology* 2012, 3.

52. Bradamante S, Barenghi L, Villa A: Cardiovascular Protective Effects of Resveratrol. *Cardiovascular Drug Reviews* 2004, 22(3):169-188.

53. Kitada M, Koya D: Renal protective effects of resveratrol. *Oxidative medicine and cellular longevity* 2013, 2013:568093.

54. Jang M, Cai L, Udeani GO, Slowing KV, Thomas CF, Beecher CW, Fong HH, Farnsworth NR, Kinghorn AD, Mehta RG: Cancer chemopreventive activity of resveratrol, a natural product derived from grapes. *Science* 1997, 275(5297):218-220.

55. Guilford JM, Pezzuto JM: Wine and Health: A Review. *American Journal of Enology and Viticulture* 2011, 62(4):471-486.

56. Delmas D, Lancon A, Colin D, Jannin B, Latruffe N: Resveratrol as a Chemopreventive Agent: A Promising Molecule for Fighting Cancer. *Current Drug Targets* 2006, 7(4):423-442.

57. Lancon A, Hanet N, Jannin B, Delmas D, Heydel JM, Lizard G, Chagnon MC, Artur Y, Latruffe N: Resveratrol in human hepatoma HepG2 cells: metabolism and inducibility of detoxifying enzymes. *Drug metabolism and disposition: the biological fate of chemicals* 2007, 35(5):699-703.

58. She QB, Ma WY, Wang M, Kaji A, Ho CT, Dong Z: Inhibition of cell transformation by resveratrol and its derivatives: differential effects and mechanisms involved. *Oncogene* 2003, 22(14):2143-2150.

59. Csiszar A, Labinskyy N, Pinto JT, Ballabh P, Zhang H, Losonczy G, Pearson K, de Cabo R, Pacher P, Zhang C: Resveratrol induces mitochondrial biogenesis in endothelial cells. *American journal of physiology Heart and circulatory physiology* 2009, 297(1):H13-20.

60. Ray PS, Maulik G, Cordis GA, Bertelli AAE, Bertelli A, Das DK: The red wine antioxidant resveratrol protects isolated rat hearts from ischemia reperfusion injury. *Free Radical Biology and Medicine* 1999, 27(1–2):160-169.

61. Luo X-Y, Qu S-L, Tang Z-H, Zhang Y, Liu M-H, Peng J, Tang H, Yu K-L, Zhang C, Ren Z: SIRT1 in cardiovascular aging. *Clinica Chimica Acta* 2014, 437(0):106-114.

62. Martinet W, Kockx MM: Apoptosis in atherosclerosis: focus on oxidized lipids and inflammation. *Current opinion in lipidology* 2001, 12(5):535-541.

63. Hsieh TC, Wu JM: Differential effects on growth, cell cycle arrest, and induction of apoptosis by resveratrol in human prostate cancer cell lines. *Experimental cell research* 1999, 249(1):109-115.

64. Momchilova A, Petkova D, Staneva G, Markovska T, Pankov R, Skrobanska R, Nikolova-Karakashian M, Koumanov K: Resveratrol alters the lipid composition, metabolism and peroxide level in senescent rat hepatocytes. *Chemico-biological interactions* 2014, 207:74-80.

65. Narayanan NK, Narayanan BA, Nixon DW: Resveratrol-induced cell growth inhibition and apoptosis is associated with modulation of phosphoglycerate mutase B in human prostate cancer cells: two-dimensional sodium dodecyl sulfate-polyacrylamide gel electrophoresis and mass spectrometry evaluation. *Cancer detection and prevention* 2004, 28(6):443-452.

66. Schneider Y, Vincent F, Duranton B, Badolo L, Gosse F, Bergmann C, Seiler N, Raul F: Anti-proliferative effect of resveratrol, a natural component of grapes and wine, on human colonic cancer cells. *Cancer letters* 2000, 158(1):85-91.

67. Tennen Ruth I, Michishita-Kioi E, Chua Katrin F: Finding a Target for Resveratrol. *Cell* 2012, 148(3):387-389.

68. Saunders LR, Verdin E: Sirtuins: critical regulators at the crossroads between cancer and aging. *Oncogene* 2007, 26(37):5489-5504.

69. Li X: SIRT1 and energy metabolism. *Acta Biochimica et Biophysica Sinica* 2013, 45(1):51-60.

70. Barger JL KT, Vann JM, Arias EB, Wang J: A Low Dose of Dietary Resveratrol Partially Mimics Caloric Restriction and Retards Aging Parameters in Mice. *PloS one* 2008, 3(6).

71. Jaiswal AK: Nrf2 signaling in coordinated activation of antioxidant gene expression. *Free Radical Biology and Medicine* 2004, 36(10):1199-1207.

72. Motohashi H, Yamamoto M: Nrf2–Keap1 defines a physiologically important stress response mechanism. *Trends in Molecular Medicine* 2004, 10(11):549-557.

73. Weydert CJ, Cullen JJ: Measurement of superoxide dismutase, catalase and glutathione peroxidase in cultured cells and tissue. *Nature protocols* 2010, 5(1):51-66.

74. Alfonso-Prieto M, Vidossich P, Rovira C: The reaction mechanisms of heme catalases: An atomistic view by ab initio molecular dynamics. *Archives of Biochemistry and Biophysics* 2012, 525(2):121-130.

75. Wu G, Fang YZ, Yang S, Lupton JR, Turner ND: Glutathione metabolism and its implications for health. *The Journal of nutrition* 2004, 134(3):489-492.

76. Li S, Yan T, Yang J-Q, Oberley TD, Oberley LW: The Role of Cellular Glutathione Peroxidase Redox Regulation in the Suppression of Tumor Cell Growth by Manganese Superoxide Dismutase. *Cancer Research* 2000, 60(14):3927-3939.

77. Zitka O, Skalickova S, Gumulec J, Masarik M, Adam V, Hubalek J, Trnkova L, Kruseova J, Eckschlager T, Kizek R: Redox status expressed as GSH:GSSG ratio as a marker for oxidative stress in paediatric tumour patients. *Oncology letters* 2012, 4(6):1247-1253.

78. Noren Hooten N, Kompaniez K, Barnes J, Lohani A, Evans MK: Poly(ADP-ribose) polymerase 1 (PARP-1) binds to 8-oxoguanine-DNA glycosylase (OGG1). *The Journal of biological chemistry* 2011, 286(52):44679-44690.

79. Riss TL MR, Niles AL, Minor L: Cell Viability Assays. *Assay Guidance Manual [Internet]* 2013.

80. Townsend DM, Tew KD, Tapiero H: The importance of glutathione in human disease. *Biomedicine & pharmacotherapy* 2003, 57(3-4):145-155.

81. Ostling O, Johanson KJ: Microelectrophoretic study of radiation-induced DNA damages in individual mammalian cells. *Biochemical and biophysical research communications* 1984, 123(1):291-298.

82. Singh NP, McCoy MT, Tice RR, Schneider EL: A simple technique for quantitation of low levels of DNA damage in individual cells. *Experimental cell research* 1988, 175(1):184-191.

83. Collins AR, Oscoz AA, Brunborg G, Gaivão I, Giovannelli L, Kruszewski M, Smith CC, Štětina R: The comet assay: topical issues. *Mutagenesis* 2008, 23(3):143-151.

84. Peake I: The polymerase chain reaction. *Journal of clinical pathology* 1989, 42(7):673-676.

85. Lynch JR, Brown JM: The polymerase chain reaction: current and future clinical applications. *Journal of medical genetics* 1990, 27(1):2-7.

86. Livak KJ, Schmittgen TD: Analysis of relative gene expression data using real-time quantitative PCR and the 2(-Delta Delta C(T)) Method. *Methods* 2001, 25(4):402-408.

87. Smith PK, Krohn RI, Hermanson GT, Mallia AK, Gartner FH, Provenzano MD, Fujimoto EK, Goeke NM, Olson BJ, Klenk DC: Measurement of protein using bicinchoninic acid. *Analytical Biochemistry* 1985, 150(1):76-85.

88. Walker JM: The bicinchoninic acid (BCA) assay for protein quantitation. *Methods in molecular biology* 1994, 32:5-8.

89. Laemmli UK: Cleavage of structural proteins during the assembly of the head of bacteriophage T4. *Nature* 1970, 227(5259):680-685.

90. Weber K, Osborn M: The reliability of molecular weight determinations by dodecyl sulfate-polyacrylamide gel electrophoresis. *The Journal of biological chemistry* 1969, 244(16):4406-4412.

91. Towbin H, Staehelin T, Gordon J: Electrophoretic transfer of proteins from polyacrylamide gels to nitrocellulose sheets: procedure and some applications. *Proceedings of the National Academy of Sciences* 1979, 76(9):4350-4354.

92. Rossi D, Guerrini A, Bruni R, Brognara E, Borgatti M, Gambari R, Maietti S, Sacchetti G: trans-Resveratrol in nutraceuticals: issues in retail quality and effectiveness. *Molecules* 2012, 17(10):12393-12405.

93. Boesch-Saadatmandi C, Loboda A, Jozkowicz A, Huebbe P, Blank R, Wolffram S, Dulak J, Rimbach G: Effect of ochratoxin A on redox-regulated transcription factors, antioxidant enzymes and glutathione-S-transferase in cultured kidney tubulus cells. *Food and chemical toxicology : an international journal published for the British Industrial Biological Research Association* 2008, 46(8):2665-2671.

94. Sasaki T, Maier B, Koclega KD, Chruszcz M, Gluba W, Stukenberg PT, Minor W, Scrable H: Phosphorylation Regulates SIRT1 Function. *PloS one* 2008, 3(12):e4020.

95. Nasrin N, Kaushik VK, Fortier E, Wall D, Pearson KJ, de Cabo R, Bordone L: JNK1 phosphorylates SIRT1 and promotes its enzymatic activity. *PloS one* 2009, 4(12):e8414.

Appendix A

1.

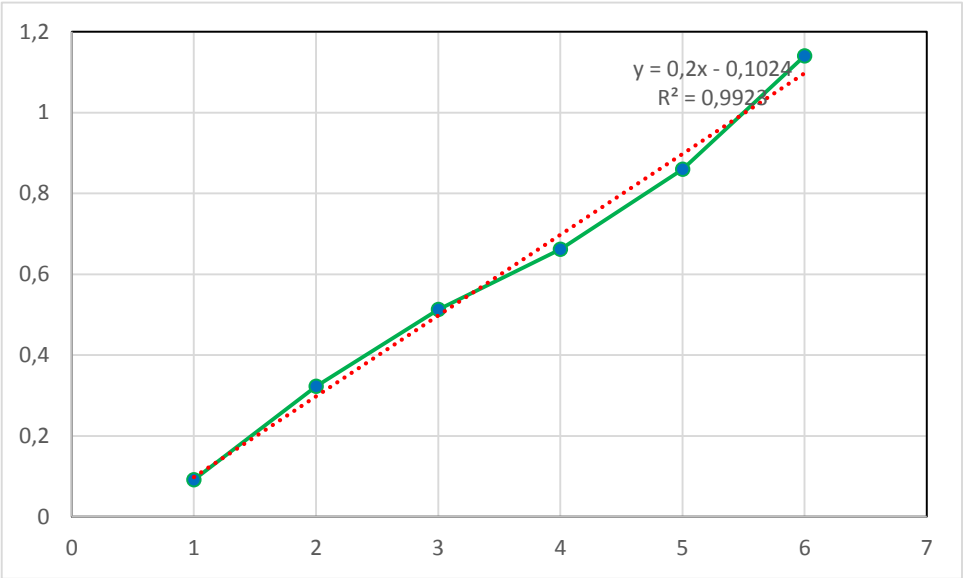

Figure 1: Standard curve using known concentrations of BSA to determine the unknown concentrations of protein samples in the BCA assay.

2.

Table 1: Calculation of protein concentrations using equation generated from standard curve and standardisation to 1.5mg/ml.

Samples	OD 1	OD 2	Average OD	Protein Conc (mg/ml)	Protein Vol (µl)	Cytobuster Vol (µl)
C	2,852	1,96	2,406	12,542	23,91963004	176,08037
V	2,472	2,403	2,4375	12,6995	23,62297728	176,3770227
O	2,71	2,055	2,3825	12,4245	24,14584088	175,8541591
CR	2,082	2,382	2,232	11,672	25,70253598	174,297464
OR	3,31	2,515	2,9125	15,0745	19,90115758	180,0988424

Appendix B

1. **Table 1**: Raw data of comet tail length measurements (μm)

C	C	O	O	R	R	OR	OR
39,99	12,9	29,67	36,12	7,74	9,03	42,57	32,25
42,57	19,35	32,25	45,15	11,61	6,45	37,41	33,54
41,28	12,9	29,67	42,57	11,61	10,32	21,93	36,12
43,86	24,51	34,83	39,99	12,9	11,61	24,51	32,25
43,86	27,09	39,99	38,7	7,74	7,74	21,93	33,54
28,38	24,51	33,54	36,12	6,45	15,48	24,51	30,96
43,86	23,22	45,15	34,83	6,45	7,74	19,35	28,38
38,7	34,83	47,73	38,7	10,32	18,06	15,48	30,96
43,86	38,7	47,73	43,86	7,74	15,48	25,8	28,38
39,99	10,32	45,15	39,99	6,45	12,9	21,93	38,7
41,28	36,12	39,99	42,57	6,45	15,48	29,67	34,83
49,02	34,83	46,44	46,44	6,45	12,9	29,67	38,7
32,25	38,7	38,7	50,31	6,45	15,48	34,83	39,99
24,51	32,25	41,28	47,73	9,03	11,61	32,25	33,54
29,67	41,28	37,41	46,44	6,45	15,48	32,25	38,7
28,38	30,96	38,7	52,89	7,74	19,35	41,28	19,35
32,25	30,96	64,5	56,76	7,74	19,35	16,77	25,8
37,41	36,12	63,21	59,34	14,19	20,64	19,35	19,35
32,25	36,12	56,76	52,89	7,74	20,64	27,09	10,32
16,77	39,99	61,92	67,08	7,74	20,64	29,67	16,77
27,09	38,7	61,92	51,6	6,45	14,19	28,38	24,51
18,06	36,12	29,67	64,5	6,45	18,06	39,99	33,54
32,25	36,12	33,54	56,76	10,32	21,93	37,41	36,12
19,35	28,38	30,96	58,05	10,32	21,93	29,67	18,06
14,19	10,32	30,96	29,67	9,03	10,32	34,83	18,06

Appendix C

1. **Table 1**: Raw data used to calculate IC_{50} of OTA.

Concentration	Log Concentration	OD 1	OD 2	OD 3	Mean OD	Percent Viability
Control	0	0,484	0,463	0,585	0,51066667	100,000
Vehicle	0	0,556	0,416	0,412	0,46133333	90,339
0.25µM	2,398	0,352	0,251	0,353	0,31866667	62,402
0.5µM	2,699	0,527	0,175	0,255	0,319	62,467
1µM	3	0,312	0,301	0,278	0,297	58,159
2µM	3,301	0,197	0,258	0,187	0,214	41,906
5µM	3,699	0,233	0,154	0,105	0,164	32,115
10µM	4	0,147	0,111	0,16	0,13933333	27,285
20µm	4,301	0,052	0,065	0,111	0,076	14,883
50µm	4,699	0,051	0,033	0,057	0,047	9,204

Appendix D

1. Table 1: Raw flow cytometry data for the measurement of intracellular ROS.

Sample	1	2	3	4	5	6	7		Avg % of IC ROS measurement
C1	53,79%	50,32%	53,79%	50,32%	53,79%	50,32%	53,79%	0,523029	52,30285714
C1	50,87%	47,92%	50,87%	47,92%	50,87%	47,92%	50,87%	0,496057	49,60571429
C1	42,49%	39,67%	42,49%	39,67%	42,49%	39,67%	42,49%	0,412814	41,28142857
O1	23,90%	22,35%	23,90%	22,35%	23,90%	22,35%	23,90%	0,232357	23,23571429
O2	27,88%	25,59%	27,88%	25,59%	27,88%	25,59%	27,88%	0,268986	26,89857143
O2	27,00%	24,62%	27,00%	24,62%	27,00%	24,62%	27,00%	0,2598	25,98
R 1	21,07%	19,49%	21,07%	19,49%	21,07%	19,49%	21,07%	0,203929	20,39285714
R 1	20,89%	19,25%	20,89%	19,25%	20,89%	19,25%	20,89%	0,201871	20,18714286
R 1	20,84%	19,25%	20,84%	19,25%	20,84%	19,25%	20,84%	0,201586	20,15857143
OR2	29,81%	28,00%	29,81%	28,00%	29,81%	28,00%	29,81%	0,290343	29,03428571
OR2	30,15%	28,28%	30,15%	28,28%	30,15%	28,28%	30,15%	0,293486	29,34857143
OR2	29,15%	27,32%	29,15%	27,32%	29,15%	27,32%	29,15%	0,283657	28,36571429

2.

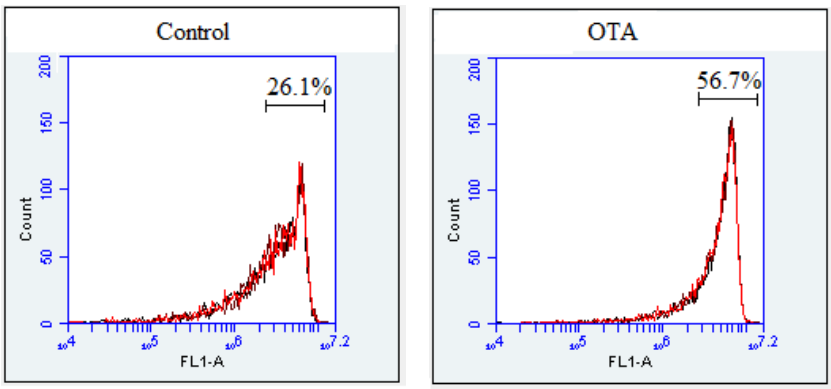

Figure 1: Scatter plots of flow cytometry data used to calculate the percentage of ROS in each sample set.